

1 YodL and YisK possess shape-modifying activities that are suppressed by mutations in *Bacillus*  
2 *subtilis mreB* and *mbl*

3

4

5 Yi Duan\*, Anthony M. Sperber\*, and Jennifer K. Herman<sup>#</sup>

6

7 Department of Biochemistry and Biophysics, Texas A&M University, College Station, TX USA

8

9 Running Header: Modulators of MreB and Mbl Activity

10

11

12 <sup>#</sup>Address correspondence to Jennifer K. Herman, [jkherman@tamu.edu](mailto:jkherman@tamu.edu)

13 \*these authors contributed equally

14

15

16

17

18

19

20

21

22

23

24 **Abstract**

25

26 Many bacteria utilize actin-like proteins to direct peptidoglycan (PG) synthesis. MreB and  
27 MreB-like proteins are thought to act as scaffolds, guiding the localization and activity of key PG  
28 synthesizing proteins during cell elongation. Despite their critical role in viability and cell-shape  
29 maintenance, very little is known about how the activity of MreB family proteins is regulated.  
30 Using a *Bacillus subtilis* misexpression screen, we identified two genes *yodL* and *yisK*, that when  
31 misexpressed lead to loss of cell width control and cell lysis. Expression analysis suggests that  
32 *yodL* and *yisK* are previously uncharacterized Spo0A-regulated genes, and consistent with these  
33 observations, a  $\Delta yodL \Delta yisK$  mutant exhibits reduced sporulation efficiency. Suppressors  
34 resistant to YodL's killing activity occurred primarily in *mreB* and resulted in amino acid  
35 substitutions at the interface between MreB and the highly conserved morphogenic protein  
36 RodZ, whereas suppressors resistant to YisK occurred primarily in *mbl*, and mapped to Mbl's  
37 predicted ATP-binding pocket. YodL's shape-altering activity appears to require MreB, as a  
38  $\Delta mreB$  mutant is resistant to the effects of YodL but not YisK. Similarly, YisK appears to  
39 require Mbl, as a  $\Delta mbl$  mutant is resistant to cell-widening effects of YisK, but not YodL.  
40 Collectively, our results suggest that YodL and YisK likely modulate MreB and Mbl activity,  
41 possibly during the early stages of sporulation.

42

43

44

## 45 **Importance**

46           The peptidoglycan (PG) component of cell envelope confers structural rigidity to bacteria  
47 and protects them from osmotic pressure. MreB and MreB-like proteins are thought to act as  
48 scaffolds for PG synthesis, and are essential in bacteria exhibiting non-polar growth. Despite the  
49 critical role of MreB-like proteins, we lack mechanistic insight into how their activities are  
50 regulated. Here, we describe the discovery of two *B. subtilis* proteins, YodL and YisK, which  
51 modulate MreB and Mbl activity. Our data suggest YodL specifically targets MreB, whereas  
52 YisK targets Mbl. The apparent specificity with which YodL and YisK are able to differentially  
53 target MreB and Mbl make them potentially powerful tools for probing the mechanics of  
54 cytoskeletal function in bacteria.

55

56

57

58

59

60

61

62

63

64

65

66

## 67 **Introduction**

68 Bacterial cell growth requires that the machineries directing enlargement and division of  
69 the bacterial cell envelope be coordinated in both time and space (1). The cell envelope is  
70 comprised of membranes and a macromolecular mesh of peptidoglycan (PG) that possesses both  
71 rigid and elastic properties (2, 3). PG is highly cross-linked, allowing bacteria to maintain  
72 shapes and avoid lysis, even in the presence of several atmospheres of internal turgor pressure.  
73 PG rearrangements are required during the inward redirection of growth that occurs at the time  
74 of cell division, but are also necessary when cells insert new PG and dynamically modify their  
75 morphologies in response to developmental or environmental signals (4, 5). To avoid lysis  
76 during PG rearrangements, bacteria must carefully regulate the making and breaking of glycan  
77 strands and peptide crosslinks (3). In rod-shaped bacteria, PG enlargement during steady-state  
78 growth is constrained in one dimension along the cell's long-axis and can either occur through  
79 polar growth, as is the case in *Agrobacterium tumefaciens* and *Streptomyces coelicolor*, or  
80 through incorporation of new cell wall material along the length of the cell cylinder, as observed  
81 in *Escherichia coli*, *Bacillus subtilis*, and *Caulobacter crescentus* (6).

82 To control cell diameter and create osmotically stable PG, bacteria that exhibit non-polar  
83 growth require the activity of the highly conserved actin-like protein MreB. Biochemical,  
84 genetic, and cell biological data suggest that MreB likely directs PG synthesis during cell  
85 elongation and in some bacteria, MreB may also function during cell division (7-9). MreB  
86 possesses ATPase activity, and polymerizes at sites along the cytoplasmic side of the inner  
87 membrane (10). ATP binding and hydrolysis is required for MreB polymerization and activity  
88 (11) and two S-benzylisothiourea derivatives, A22 and MP265, target the ATPase domain of  
89 MreB in Gram negative organisms, possibly preventing nucleotide hydrolysis and/or release (12-

90 15). Depletion or inactivation of MreB is lethal except in some conditional backgrounds (16,  
91 17), so organisms sensitive to A22 and/or MP265 lose shape and eventually lyse (12-15).

92 MreB has been found to interact with several other proteins involved in PG synthesis,  
93 including the bitopic membrane protein RodZ (8, 16, 18-20). RodZ interacts directly with MreB  
94 through a cytoplasmic helix-turn-helix motif located at its N-terminus (18). A co-crystal  
95 structure of RodZ and MreB shows the N-terminus of RodZ extending into a conserved  
96 hydrophobic pocket located in subdomain IIA of MreB (18). Depletion of RodZ also leads to  
97 loss of cell shape and cell death (21-23). However, in various mutant backgrounds, *rodZ* can be  
98 deleted without loss of rod shape or viability, indicating that RodZ is not absolutely required for  
99 MreB's function in maintaining shape (24-26). Based on these observations and others, it has  
100 been proposed that MreB-RodZ interactions may regulate some aspect of MreB activity (10, 26).

101 Gram-positives often encode multiple paralogs (27). *B. subtilis* possesses three *mreB*  
102 family genes: *mreB*, *mbl*, and *mreBH*. *mreB* is distinguished from *mbl* and *mreBH* by its  
103 location within the highly conserved *mreBCD* operon. Although *mreB*, *mbl*, and *mreBH* are  
104 essential, it has been reported that each can be deleted under conditions in which cells are  
105 provided sufficient magnesium (28-30), or in strain backgrounds lacking *ponA*, the gene  
106 encoding penicillin binding protein 1 (PBPI) (20). In addition, all three genes can be deleted in  
107 a single background with only minor effects on cell shape if any one of the paralogs is artificially  
108 overexpressed in *trans* from an inducible promoter (31). The ability of any one of the paralogs  
109 to compensate for the loss of the others, at least under some growth conditions, strongly suggests  
110 that MreB, Mbl, and MreBH share significant functional redundancy (31, 32).

111 At the same time, several lines of evidence suggest that the paralogs possess non-  
112 overlapping functions. The genes themselves exhibit different patterns of transcriptional

113 regulation, suggesting that each likely possesses specialized activities that are important in  
114 different growth contexts. For example, *mreB* and *mbl* are maximally expressed at the end of  
115 exponential growth, but expression falls off sharply during stationary phase (33), whereas  
116 *mreBH* is part of the SigI heat-shock regulon (34). There is also evidence suggesting that each  
117 protein may possess specialized activities. For example, MreBH interacts with the lytic  
118 transglycosylase LytE, and is required for LytE localization (35), whereas the lytic  
119 transglycosylase CwLO, depends on Mbl for wildtype function (35). More recently MreB (but  
120 not Mbl or MreBH) was shown to aid in escape from the competent cell state (33).

121       Aside from RodZ (10, 26), only a handful of proteins targeting MreB activity in vivo  
122 have been identified. In *E. coli*, the YeeU-YeeV prophage toxin-antitoxin system is comprised  
123 of a negative regulator of MreB polymerization, CbtA (36), and a positive regulator of MreB  
124 bundling, CbeA (37). Another *E. coli* prophage toxin, CptA, is also reported to inhibit MreB  
125 polymerization (38). The MbiA protein of *C. crescentus* appears to regulate MreB in vivo,  
126 however, its physiological role is unknown (39). Given the importance of PG synthesis to cell  
127 viability and in cell shape control, it is likely that many undiscovered factors exist that modulate  
128 the activity of MreB and its paralogs.

129       In the present work we describe the identification of YodL and YisK, modulators of  
130 MreB and Mbl activity that are expressed during early stages of *B. subtilis* sporulation.  
131 Misexpression of either *yodL* or *yisK* during vegetative growth results in loss of cell width  
132 control and cell death. Genetic evidence indicates that YodL targets and inhibits MreB activity,  
133 whereas YisK targets and inhibits Mbl. Our data also show that YisK activity affects cell length  
134 control through an Mbl and MreBH-independent pathway.

135

## 136 **Materials And Methods**

137 **General methods.** All *B. subtilis* strains were derived from *B. subtilis* 168. *E. coli* and *B.*  
138 *subtilis* strains utilized in this study are listed in Table S2. Plasmids are listed in Table S3.  
139 Oligonucleotide primers are listed in Table S4. Details on plasmid and strain construction can be  
140 found in the Supplementary text. *Escherichia coli* DH5 $\alpha$  was used for cloning. All *E. coli*  
141 strains were grown in LB-Lennox medium supplemented with 100  $\mu$ g/ml ampicillin. The  
142 following concentrations of antibiotics were used for generating *B. subtilis* strains: 100  $\mu$ g/ml  
143 spectinomycin, 7.5  $\mu$ g/ml chloramphenicol, 0.8 mg/ml phleomycin, 10  $\mu$ g/ml tetracycline, 10  
144  $\mu$ g/ml kanamycin. To select for erythromycin resistance, plates were supplemented with 1  $\mu$ g/ml  
145 erythromycin (*erm*) and 25  $\mu$ g/ml lincomycin. *B. subtilis* transformations were carried out as  
146 described previously (40). When indicated, the LB in the *B. subtilis* microscopy experiments was  
147 LB-Lennox broth. Sporulation by resuspension was carried out at 37°C according to the Sterlini-  
148 Mandelstam method (41). Penassay broth (PAB) is composed of 5 g peptone, 1.5 g beef extract,  
149 1.5 g yeast extract, 1.0 g D-glucose (dextrose), 3.5 g NaCl, 3.68 g dipotassium phosphate, and  
150 1.32 g monopotassium phosphate per liter of distilled water. To make solid media, the relevant  
151 media was supplemented with 1.5% (w/v) bacto-agar.

152  
153 **Microscopy.** For microscopy experiments, all strains were grown in the indicated medium in  
154 volumes of 25 ml in 250 ml baffled flasks, and placed in a shaking waterbath set at 37°C and 280  
155 rpm. Unless stated otherwise, misexpression was performed by inducing samples with 1.0 mM  
156 isopropyl-beta-D-thiogalactopyranoside (IPTG) and imaging samples 90 min post-induction.  
157 Fluorescence microscopy was performed with a Nikon Ti-E microscope equipped with a CFI  
158 Plan Apo lambda DM 100X objective, Prior Scientific Lumen 200 Illumination system, C-FL

159 UV-2E/C DAPI and C-FL GFP HC HISN Zero Shift filter cubes, and a CoolSNAP HQ2  
160 monochrome camera. Membranes were stained with TMA-DPH [1-(4-  
161 trimethylammoniumphenyl)-6-phenyl-1,3,5-hexatriene *p*-toluenesulfonate] (0.02 mM) and  
162 imaged with exposure times of 1 sec with a neutral density filter in place to reduce cytoplasmic  
163 background. All GFP images were captured with a 1 sec exposure time. All images were  
164 captured with NIS Elements Advanced Research (version 4.10), and processed with NIS  
165 Elements Advanced Research (version 4.10) and ImageJ64 (42). Cells were mounted on glass  
166 slides with 1% agarose pads or polylysine-treated coverslips prior to imaging. To quantitate cell  
167 lengths for Fig 5, the cell lengths for 500 cells were determined for each population. The  
168 statistical significance of cell length differences between populations was determined using an  
169 unpaired student's t-test.

170

171 **Plate growth assays.** *B. subtilis* strains were streaked on LB-Lennox plates containing 100  
172  $\mu\text{g/ml}$  spectinomycin and 1 mM IPTG. The plates were supplemented with the indicated  
173 concentrations of  $\text{MgCl}_2$  when indicated. Plates were incubated at 37°C overnight and images  
174 were captured on a ScanJet G4050 flatbed scanner (Hewlett Packard).

175

176 **Heat Kill.** Spore formation was quantified by growing cells in Difco sporulation medium  
177 (DSM)(43). A freshly grown single colony of each strain was inoculated into 2 mL of DSM  
178 media and placed in a roller drum at 37°C, 60 rpm for 36 hrs. To determine colony forming  
179 units/ml, an aliquot of each culture was serially diluted and plated on DSM agar plates. To  
180 enumerate heat resistant spores/ml, the serial diluted cultures were subjected to a 20 min heat  
181 treatment at 80°C and plated on DSM agar plates. The plates were incubated at 37°C overnight



182 and the next day colony counts were determined. The relative sporulation frequency compared  
183 to wildtype was determined by calculating the spores/CFU of each experimental and dividing it  
184 by the spores/CFU of wildtype. The reported statistical significance was determined using an  
185 unpaired student's t-test.

186

187 **Transcriptional fusions.** Transcriptional fusions were constructed by fusing a ~200 bp region  
188 up to the start codon of either *yodL* or *yisK* to *gfp* or *lacZ* and integrating the fusions into the *B.*  
189 *subtilis* chromosome at the *amyE* locus (for more details, see strain construction in the  
190 supplemental text). Microscopy was conducted on each strain over a timecourse in sporulation  
191 by resuspension media (see general methods) or in a nutrient exhaustion timecourse in CH (44).  
192 Beta-galactosidase assays were performed as described (45), except all samples were frozen at -  
193 80°C before processing. All experiments were performed on at least three independent  
194 biological replicates.

195

196 **Suppressor selections.** Single colonies of BYD048 (3X  $P_{hy}$ -*yodL*,  $P_{hy}$ -*lacZ*) or BYD076 (3X  
197  $P_{hy}$ -*yisK*,  $P_{hy}$ -*lacZ*) were used to inoculate independent 5 ml LB-Lennox cultures. Six  
198 independent cultures were grown for each strain. The cultures were grown for 6 hrs at 37°C and  
199 0.3  $\mu$ l of each culture was diluted in 100  $\mu$ l LB and plated on an LB-Lennox agar plate  
200 containing 100  $\mu$ g/ml spectinomycin and 1 mM isopropyl- $\beta$ -D-thiogalactopyranoside (IPTG).  
201 After overnight growth, suppressors that arose were patched on both LB-Lennox agar plates  
202 supplemented with 100  $\mu$ g/ml spectinomycin and LB-Lennox agar plates supplemented with 100  
203  $\mu$ g/ml spectinomycin, 1.0 mM isopropyl- $\beta$ -D-thiogalactopyranoside (IPTG), and 40  $\mu$ g/ml X-Gal  
204 and grown at 37°C overnight. Only blue colonies were selected for further analysis; this screen

205 eliminated mutants unable to derepress  $P_{hy}$  in the presence of IPTG. In addition, each  $P_{hy-yodL}$   
206 or  $P_{hy-yisK}$  construct was transformed into a wildtype background to ensure that the construct  
207 remained fully functional with respect to preventing cell growth on LB-Lennox agar plates  
208 supplemented with the relevant antibiotic and 1 mM isopropyl- $\beta$ -D-thiogalactopyranoside  
209 (IPTG).

210

211 **Whole-genome sequencing and analysis.** Genomic DNA was isolated from six YodL-resistant  
212 suppressors obtained from independent cultures as well as the parent strain (BYD048) by  
213 inoculating a single colony in 6 ml LB-Lennox media and growing at 37°C for 4 hr in a roller  
214 drum. Cells were collected by spinning at 21,130 x g for 2 min at room temperature,  
215 resuspending the pellets in lysis buffer [20 mM Tris-HCl pH 7.5, 50 mM EDTA pH 8, 100 mM  
216 NaCl, and 2 mg/ml lysozyme] and incubing at 37°C for 30 min. Sarkosyl was added to a final  
217 concentration of 1% (w/v). Protein was removed by extracting with 600  $\mu$ l phenol, centrifuging  
218 at 21,130 x g for 5 min at room temperature, and transferring the top (aqueous layer) to a new  
219 microcentrifuge tube. This was followed by an extraction with 600  $\mu$ l phenol-saturated  
220 chloroform and centrifugation at 21,130 x g for 5 min at room temperature. After transferring  
221 the aqueous layer to a new microcentrifuge tube, a final extraction was performed with 100%  
222 chloroform, followed by centrifugation at 21,130 x g for 5 min at room temperature. The  
223 aqueous layer was transferred to a new microcentrifuge tube, being careful to avoid the  
224 interphase material. To precipitate the genomic DNA, a 1/10<sup>th</sup> volume of 3.0 M Na-acetate and 1  
225 ml of 100% ethanol was added, and the tube was inverted multiple times. The sample was  
226 centrifuged at 21,130 x g for 1 min at room temperature in a microcentrifuge. The pellet was  
227 washed with 150  $\mu$ l 70% ethanol and resuspended in 500  $\mu$ l TE [10 mM Tris pH 7.5, 1 mM

228 EDTA, pH 8.0]. To eliminate potential RNA contamination, RNase was added to a final  
229 concentration of 200 µg/ml and the sample was incubated at 55°C for 1 hr. To remove the  
230 RNase, the genomic DNA was re-purified by phenol-chloroform extraction and ethanol  
231 precipitation as described above. The final pellet was resuspended in 100 µl TE. Bar-coded  
232 libraries were prepared from each genomic DNA sample using a TruSeq DNA kit according to  
233 manufacture specifications (Illumina), and the samples were subjected to Illumina-based whole-  
234 genome sequencing using a MiSeq 250 paired-end run (Illumina). CLC Genomics Workbench  
235 (Qiagen) was used to map the sequence reads against the Bs168 reference genome and to  
236 identify single nucleotide polymorphisms, insertions, and deletions. Mutations associated with  
237 the  $P_{hy}$  integration constructs and those in which less than 40% of the reads differed from the  
238 reference genome were excluded as candidate changes responsible for suppression in our initial  
239 analysis (Table S1). The remaining suppressors mutations were identified by PCR amplifying  
240 *mreB* (using primer set OAS044 and OAS045) and *mbl* (using primer set OAS046 and OAS047),  
241 and sequencing with the same primers. To determine if the candidate suppressors alleles  
242 identified were sufficient to confer resistance to the original selective pressure, each was linked  
243 to a kanamycin resistance cassette and moved by transformation into a clean genetic background  
244 (see supplemental Strain Construction).

245

## 246 **Results**

247

### 248 **YodL and YisK affect cell width**

249

250 To identify novel factors involved in cellular morphogenesis, we created an ordered gene  
251 misexpression library comprising over 800 previously uncharacterized genes from *B. subtilis*.  
252 Each gene was placed under the control of an IPTG-inducible promoter ( $P_{hy}$ ) and integrated in

253 single copy (1X) at *amyE*, a non-essential locus in the *B. subtilis* chromosome. The library  
254 (called the BEIGEL for *Bacillus Ectopic Inducible Gene Expression Library*), was screened for  
255 misexpression phenotypes that perturbed growth on solid media, and also resulted in obvious  
256 defects in nucleoid morphology, changes in cell division frequency, and/or perturbations in  
257 overall cell shape in liquid cultures. Two strains, one harboring  $P_{hy}$ -*yodL* and one harboring  $P_{hy}$ -  
258 *ysisK*, were unable to form colonies on plates containing inducer (Fig 1A) and also produced  
259 wide, irregular cells with slightly tapered poles following misexpression in LB liquid media (Fig  
260 1B). Cell lysis and aberrant cell divisions were also observed. Introducing a second copy (2X)  
261 of each  $P_{hy}$  misexpression construct into the chromosome did not appreciably enhance cell  
262 widening at the 90 min post-induction timepoint, although cell lysis was more readily observed  
263 (Fig 1B).  $P_{hy}$ -*ysisK* (2X) misexpression also led to a drop in optical density over time (Fig S1A),  
264 consistent with the cell lysis observed microscopically. We conclude that the activities of *yodL*  
265 and *ysisK* target one or more processes integral to width control during cell elongation.

266         The *yodL* and *ysisK* misexpression phenotypes are similar to those observed when proteins  
267 involved in cell elongation are perturbed in *B. subtilis* (20, 31, 46). Since the addition of  
268 magnesium was previously reported to suppress the lethality and/or morphological phenotypes  
269 associated with depletion or deletion of some proteins important for cell elongation in *B. subtilis*  
270 (16, 20, 29, 31, 47), we assessed if the  $P_{hy}$ -*yodL* and  $P_{hy}$ -*ysisK* misexpression phenotypes could be  
271 rescued by growing cells with media supplemented with two different concentrations of MgCl<sub>2</sub>.  
272 The YodL-producing cells failed to grow on any LB media containing inducer, regardless of  
273 MgCl<sub>2</sub> concentration (Fig 1A). In contrast, LB supplemented with 25 mM MgCl<sub>2</sub> restored  
274 viability to the strain producing YisK (Fig 1A). Interestingly, even 25 mM MgCl<sub>2</sub> was not  
275 sufficient to suppress the cell-widening effect associated with YodL and YisK misexpression

276 (Fig 1B), although these cells did not lyse (Fig S1C). Since PAB medium was often used in the  
277 prior studies showing MgCl<sub>2</sub> supplementation rescued cell shape (16, 20, 29, 31, 47), we also  
278 assayed for growth on PAB following YodL and YisK expression. PAB supplemented with 25  
279 mM MgCl<sub>2</sub> rescued growth on plates (Fig S2A), but still did not rescue morphology in liquid  
280 culture (Fig S2B).

281

### 282 ***yodL* and *yisK* expression**

283 To better understand the possible physiological functions of the *yodL* and *yisK* gene  
284 products, we analyzed the genes and their genetic contexts bioinformatically. *yodL* is predicted  
285 to encode a 12.5 kDa hypothetical protein which, based on amino acid similarity, is conserved in  
286 the *Bacillus* genus. In data from a global microarray study analyzing conditional gene  
287 expression in *B. subtilis*, *yodL* is expressed as a monocistronic mRNA, exhibiting peak  
288 expression ~2 hrs after entry into sporulation (48). *yodL* expression is most strongly correlated  
289 with expression of *racA* and *refZ* (*yttP*) (48), genes directly regulated by Spo0A (49). *yodL* was  
290 not previously identified as a member of the Spo0A regulon controlling early sporulation gene  
291 expression (49, 50), however a more recent study found that *yodL* expression during sporulation  
292 is reduced in a  $\Delta spo0A$  mutant (51). Consistent with this observation, we identified a putative  
293 Spo0A box approximately ~75 bp upstream of the annotated *yodL* start codon (Fig 2A). *yisK* is  
294 predicted to encode a 33 kDa protein and is annotated as a putative catabolic enzyme based on its  
295 similarity to proteins involved in the degradation of aromatic amino acids (52). *yisK* was  
296 previously identified as a member of the SigH regulon, and possesses a SigH -35/-10 motif  
297 (50)(Fig 2B). Expression of *yisK* peaks ~2 hrs after entry into sporulation (39) and is most  
298 strongly correlated with expression of *kinA* (48), a gene regulated by both SigH (the stationary

299 phase sigma factor)(50, 53-55) and Spo0A (49, 56). As with *yodL*, we identified a putative  
300 Spo0A box in the regulatory region upstream of the *yisK* start codon (Fig 2B).

301 To independently test if *yodL* and *yisK* expression are consistent with Spo0A-dependent  
302 regulation, we fused the putative regulatory regions upstream of each gene to a *gfp* reporter gene,  
303 and integrated the fusions into the *amyE* locus. We then followed expression from the promoter  
304 fusions over a timecourse in CH liquid broth, a rich medium in which the cells first grow  
305 exponentially, transition to stationary phase, and finally gradually enter sporulation (Fig 3A-3C).  
306 In this timecourse, GFP signal from *P<sub>yisK</sub>-gfp* increased dramatically from time 0 (OD<sub>600</sub> ~0.6) to  
307 time 1 hr (OD<sub>600</sub> ~1.6)(Fig 3C), consistent with *yisK*'s prior characterization as a SigH-regulated  
308 gene (50). In contrast, GFP fluorescence from *P<sub>yodL</sub>-gfp* became evident at a later timepoint (120  
309 min) and was more heterogeneous (Fig 3C), consistent with expression patterns previously  
310 observed for other Spo0A-P regulated genes (57, 58).

311 To quantitate expression from the promoters, we generated *P<sub>yodL</sub>-lacZ* and *P<sub>yisK</sub>-lacZ*  
312 reporter strains and collected samples over a CH timecourse beginning with early exponential  
313 (OD<sub>600</sub> = 0.2). Expression from *P<sub>yodL</sub>-lacZ* rose steadily beginning about 2 hrs after exit from  
314 exponential growth, and continued to rise at least until the final timepoint taken (Fig 3D). In  
315 contrast, expression from *P<sub>yisK</sub>-lacZ* rose as cells transitioned from early to late exponential  
316 growth, reached peak levels shortly after exit from exponential growth, and remained steady for  
317 the remainder of the timepoints (Fig 3E). Wildtype expression from both *P<sub>yodL</sub>-lacZ* and *P<sub>yisK</sub>-*  
318 *lacZ* required both SigH and Spo0A, and was largely eliminated in the absence of both regulators  
319 (Fig 3D and 3E). We did not attempt to draw further conclusions from this data, since Spo0A  
320 and SigH each require the other for wildtype levels of expression (see discussion).

321 We then followed expression from the promoter fusions over a timecourse following the  
322 sporulation by resuspension method, which generates a more synchronous entry into sporulation  
323 (59). At time 0, neither the strain harboring  $P_{yodL}$ -*gfp*, nor the strain harboring  $P_{yisK}$ -*gfp* showed  
324 appreciable levels of fluorescence (Fig 4A), appearing similar to a negative control harboring *gfp*  
325 without a promoter (Fig S3). Between 0 and 40 min, both strains showed detectable increases in  
326 fluorescence. At 60 min, when the first polar divisions characteristic of sporulation begin to  
327 manifest, both strains were more strongly fluorescent (Fig 4A). GFP fluorescence from  $P_{yodL}$   
328 was qualitatively more intense than fluorescence produced from  $P_{yisK}$  (all images were captured  
329 and scaled with identical parameters to allow for direct comparison). Moreover, the GFP signal  
330 continued to accumulate in the strain harboring  $P_{yodL}$ -*gfp* for at least two hrs (Fig 4A) and was  
331 heterogenous, consistent with activation by Spo0A. In contrast, the fluorescence signal produced  
332 from  $P_{yisK}$ -*gfp* was similar across the population and appeared similar at the 60 and 120 min  
333 timepoints (Fig 4A), consistent with SigH regulation.

334 To quantitate expression from the promoters during a sporulation by resuspension  
335 timecourse, we collected timepoints from strains harboring either the  $P_{yodL}$ -*lacZ* or  $P_{yisK}$ -*lacZ*  
336 reporter constructs and performed beta-galactosidase assays. Expression from  $P_{yodL}$ -*lacZ* rose  
337 rapidly between the 40 min and 100 min timepoints, and steadily declined thereafter (Fig 4B).  
338 The decline in signal was not observed for the GFP reporter, likely because the GFP is stable  
339 once synthesized (60). In contrast, expression from  $P_{yisK}$ -*lacZ* was highest at the time of  
340 resuspension (T0) and declined up until the final timepoint (Fig 4C).

341 Collectively, the patterns expression we observe for *yodL* are consistent with those  
342 observed for genes activated by high-threshold levels of Spo0A during sporulation, including  
343 *racA*, *spoIIIG*, and *spoIIIA* (61). In contrast, *yisK*'s expression pattern is similar to that observed

344 for *kinA* (48, 54, 62), with expression increasing in late exponential and stationary phase and  
345 early sporulation in a SigH-dependent manner (Fig 3), but decreasing during a sporulation by  
346 resuspension timecourse (Fig 4). We do not exclude the possibility that YodL and YisK might  
347 also function in other growth contexts.

348

### 349 **A $\Delta yodL \Delta yisK$ mutant is defective in sporulation**

350 Since *yodL* and *yisK* expression correlates with other early sporulation genes, we next  
351 investigated if the gene products influenced the production of heat-resistant spores. To  
352 determine the number of heat-resistant spores in a sporulation culture, we quantified the number  
353 of colony forming units (CFU) present in cultures before (total CFU) and after (heat-resistant  
354 CFU) a heat treatment that kills vegetative cells. These values were normalized to display the  
355 sporulation efficiency of the mutants relative to wildtype. Single mutants in which either *yodL*  
356 or *yisK* were deleted displayed only mild (97% and 94%, respectively) reductions in relative  
357 sporulation efficiency (Table 1). Although the single mutants always sporulated less efficiently  
358 than wildtype in each experimental replicate, the differences were not statistically significant  
359 with only six experimental replicates. In contrast, the  $\Delta yodL \Delta yisK$  double mutant produced  
360 ~20% less heat-resistant spores than wildtype ( $P < 0.0006$ ) (Table 1). No decrease in total CFU  
361 was observed for any of the mutants compared to wildtype, indicating that the reduction in heat-  
362 resistant spores in the  $\Delta yodL \Delta yisK$  mutant was not due to reduced cell viability before heat  
363 treatment (Table 1). The gene downstream of *yisK*, *yisL*, is transcribed in the same direction as  
364 *yisK*. To determine if the reduction in sporulation we observed might be partially attributable to  
365 polar effects of the *yisK* deletion on *yisL* expression, we introduced  $P_{yisK}$ -*yisK* at an ectopic locus  
366 (*amyE*) in the  $\Delta yodL \Delta yisK$  mutant and repeated the heat-kill assay. The ectopic copy of  $P_{yisK}$ -



367 *yisK* restored sporulation in the  $\Delta yodL \Delta yisK$  to levels statistically indistinguishable from the  
368  $\Delta yodL$  single mutant (Table 1). These results lend support to the idea that YodL and YisK  
369 function during early sporulation and possess activities that, directly or indirectly, affect the  
370 production of viable spores. We do not exclude the possibility that YodL and YisK might also  
371 function outside the context of sporulation.

372         Given that *yisK* and *yodL* expression during vegetative growth leads to cell widening, we  
373 hypothesized that *yisK* and *yodL* mutants might produce thinner cells or spores during  
374 sporulation. However, no qualitative differences in cell or spore width were observed for the  
375  $\Delta yodL$ ,  $\Delta yisK$ , or  $\Delta yodL \Delta yisK$  mutant populations compared to wildtype during a sporulation  
376 timecourse (Fig S4). We also observed no qualitative differences in the shapes of germinating  
377 cells (data not shown). Thus, although YodL and YisK contribute to the production of heat-  
378 resistant spores, they do not appear to be required to generate any of the major morphological  
379 changes required for spore production.

380

### 381 **MreB and Mbl are genetic targets of YodL and YisK activity**

382

383         To identify genetic targets associated with YodL and YisK activity, we took advantage of  
384 the fact that misexpression of the proteins during vegetative growth prevents colony formation  
385 on plates and performed suppressor selection analysis. Strains harboring three copies of each  
386 misexpression cassette were utilized to reduce the chances of obtaining trivial suppressors in the  
387 misexpression cassette itself. In addition,  $P_{hy-lacZ}$  was used as a reporter to eliminate  
388 suppressors unable to release LacI repression following addition of inducer. In total, we  
389 obtained 14 suppressors resistant to YodL expression and 13 suppressors resistant to YisK  
390 expression. Six of the suppressors resistant to YodL were subjected to whole-genome

391 sequencing. The results of the sequencing are shown in Table S1. All of the suppressors  
392 possessed mutations in either *mreB* or *mbl*, genes previously shown to be important in regulating  
393 cell width (Table S1). Using targeted sequencing, we determined that the remaining suppressor  
394 strains resistant to YodL also harbored mutations in *mreB* or *mbl*. Since the phenotypes of YodL  
395 and YisK expression were similar, we also performed targeted sequencing of the *mreB* and *mbl*  
396 chromosomal regions in the YisK-resistant suppressors. All but one of the YisK-resistant  
397 suppressors possessed mutations in *mbl*; the remaining suppressor harbored a mutation in *mreB*.

398 To determine if the point mutations we identified were sufficient to confer resistance to  
399 YodL or YisK misexpression, we generated the mutant alleles in clean genetic backgrounds (see  
400 Supplementary text) and assayed for resistance to three copies (3X) of each misexpression  
401 construct (Table 2). In all cases but one, the engineered strains were resistant to the same  
402 selective pressure applied in the original selections (either 3X *yodL* or 3X *yisK*)(Table 2),  
403 indicating that the *mreB* or *mbl* mutations identified through sequencing were sufficient to confer  
404 resistance. When we attempted to engineer a strain harboring only MreB<sub>S154R</sub>, all but one of the  
405 strains also possessed a second substitution, MreB<sub>R230C</sub>. Although the remaining strain possessed  
406 only the MreB<sub>S154R</sub> substitution in MreB, unlike the original suppressor identified by whole  
407 genome sequencing (Table S1), the MreB<sub>S154R</sub> harboring strain was also sensitive to YodL  
408 expression. Based on these data, we suspect that the strain harboring MreB<sub>S154R</sub> might be  
409 unstable, and possibly predisposed to the accumulation of second-site mutations.

410 The YodL-resistant strains generally possessed mutations resulting in amino acid  
411 substitutions with charge changes (Table 2). When mapped to the *T. maritima* MreB structure,  
412 5/7 of the unique suppressor strains possessed amino acid substitutions in a region important for  
413 mediating the interaction between MreB and the bitopic membrane protein RodZ (MreB<sub>G143A</sub>,

414 MreB<sub>N145D</sub>, MreB<sub>P147R</sub>, MreB<sub>S154R</sub>, and MreB<sub>R282S</sub>(Table 2 and Fig S5)(18, 63); three of these  
415 substitutions occur in residues that make up the RodZ-MreB binding surface (MreB<sub>N140</sub>,  
416 MreB<sub>P142</sub>, and MreB<sub>R279</sub> in *T. maritima*)(18).

417 A majority of the YisK-resistant Mbl variants clustered in regions of Mbl that are  
418 predicted to make up the ATP-binding pocket (Table 2 and Fig S6). Moreover, seven of the  
419 substitutions occurred in amino acids previously associated with resistance to the MreB inhibitor  
420 A22 in *C. crescentus* and *Vibrio cholerae* (Fig S6)(12, 64, 65).

421 MreB<sub>R117G</sub> and Mbl<sub>E250K</sub> were independently isolated in both the YodL and YisK  
422 suppressor selections, raising the possibility that at least some of the other MreB and Mbl  
423 variants might exhibit cross-resistance to YodL and YisK misexpression. To test for cross-  
424 resistance, we generated the mutant alleles in clean genetic backgrounds, and then introduced 3X  
425 copies of P<sub>hy</sub>-yisK into the YodL-resistant suppressors, and 3X copies P<sub>hy</sub>-yodL into the YisK-  
426 resistant suppressors. We then assayed for the ability of the misexpression strains to grow on  
427 media in the presence of inducer. The results, summarized in Table 2, show that several of the  
428 variants exhibited resistance to both YodL and YisK. Three MreB variants, MreB<sub>N145D</sub>,  
429 MreB<sub>P147R</sub> and MreB<sub>R282S</sub>, exhibited specificity in their resistance to YodL compared to YisK.  
430 Three Mbl variants, Mbl<sub>R63C</sub>, Mbl<sub>ΔS251</sub>, and Mbl<sub>P309L</sub>, showed specificity in their resistance to  
431 YisK over YodL. These results suggest that the alleles exhibiting cross-resistance to both YisK  
432 and YodL are likely to be general, possibly conferring gain-of-function to either MreB or Mbl  
433 activity.

434

435 **YodL and YisK's cell-widening activities require MreB and Mbl, respectively**

436

437 The phenotypic consequences of YodL and YisK misexpression are similar but not  
438 identical (Fig 1B), suggesting that YodL and YisK might have distinct targets. Consistent with  
439 this idea, YodL and YisK coexpression resulted in phenotypes distinct from misexpression of  
440 either YodL or YisK alone. More specifically, cells co-expressing YodL and YisK did not grow  
441 on plates, regardless of media or MgCl<sub>2</sub> concentration (Fig 5A and Fig S2A) and growth without  
442 lysis in liquid media required the presence of MgCl<sub>2</sub> (Fig S1, Fig S2B, and Fig 5B). Importantly,  
443 the co-expressing cells displayed a round morphology that strongly contrasted with strains  
444 expressing either YodL or YisK alone (Fig 5B and Fig S2B). The round morphology was  
445 unlikely due to higher expression of gene products (1X P<sub>hy-yodL</sub> plus 1X P<sub>hy-yisK</sub>), since cells  
446 harboring two copies (2X) of either P<sub>hy-yodL</sub> or P<sub>hy-yisK</sub> did not become round (Fig 1B and Fig  
447 S2B).

448 Based on the observation that YodL and YisK coexpression yields distinct phenotypes,  
449 and the fact that all of the YodL-specific suppressor mutations occurred in *mreB* (MreB<sub>N145D</sub>,  
450 MreB<sub>P147R</sub> and MreB<sub>R282S</sub>), while all of the YisK-specific suppressor mutations occurred in *mbl*  
451 (Mbl<sub>R63C</sub>, Mbl<sub>ΔS251</sub>, and Mbl<sub>P309L</sub>), we hypothesized that YodL targets MreB, whereas YisK  
452 targets Mbl. To test these hypotheses, we assessed if MreB and Mbl are specifically required for  
453 YodL and YisK function by taking advantage of the fact that *mreB* and *mbl* can be deleted in a  
454  $\Delta$ *ponA* background with only minor changes in cell shape (20, 31). The  $\Delta$ *ponA* strain, which  
455 does not make PBP1, produces slightly longer and thinner cells than the parent strain, and  
456 requires MgCl<sub>2</sub> supplementation for normal growth (66, 67). We generated  $\Delta$ *ponA*  $\Delta$ *mreB* and  
457  $\Delta$ *ponA*  $\Delta$ *mbl* strains and then introduced either two copies of P<sub>hy-yodL</sub> or two copies of P<sub>hy-yisK</sub>  
458 into each background. We reasoned that 2X expression would provide a more stringent test for  
459 specificity than 1X expression, as off-target effects (if any), would be easier to detect. To assess

460 the requirement of either *mreB* or *mbl* for YodL and YisK activity, cells were grown to  
461 exponential phase in LB media supplemented with 10 mM MgCl<sub>2</sub>, back-diluted to a low optical  
462 density, and induced for 90 min before images were captured for microscopy. Uninduced  
463 controls all appeared as regular rods, although  $\Delta$ *ponA* deletion strains were noticeably thinner  
464 than wildtype parents (Fig 6). The  $\Delta$ *ponA* cells became wider following YodL expression,  
465 indicating that PBP1 is not required for YodL activity. We also observed that the poles of the  
466  $\Delta$ *ponA* mutant were less elongated and tapered than the wild-type control following YodL  
467 expression, suggesting that this particular effect of YodL expression is PBP1-dependent (Fig  
468 6A). A  $\Delta$ *ponA*  $\Delta$ *mbl* mutant phenocopied the  $\Delta$ *ponA* parent following YodL expression (Fig  
469 6A), indicating that Mbl is not required for YodL's activity. In contrast, the  $\Delta$ *ponA*  $\Delta$ *mreB* strain  
470 did not show morphological changes following YodL expression, and instead appeared similar to  
471 the uninduced control. We conclude that YodL requires MreB for its cell-widening activity.

472 We performed a similar series of experiments for YisK misexpression. The  $\Delta$ *ponA*  
473 mutant was sensitive to YisK expression, indicating that PBP1 is not required for YisK-  
474 dependent cell-widening. Similarly, expression of YisK in a  $\Delta$ *ponA*  $\Delta$ *mreB* mutant also resulted  
475 in loss of cell width control (Fig 6B), indicating that MreB is not required for YisK activity;  
476 however, unlike YisK expression in a wildtype or  $\Delta$ *ponA* background, the cells became round  
477 (Fig 6B), more similar to the YodL and YisK co-expressing cells (Fig 5 and Fig S2B). In  
478 contrast, a  $\Delta$ *ponA*  $\Delta$ *mbl* mutant did not lose control over cell width following YisK expression  
479 (Fig 6B), indicating that YisK activity requires Mbl for its cell-widening activity. We conclude  
480 that YodL requires MreB, but not Mbl for its cell-widening activity, whereas YisK requires Mbl,  
481 but not MreB.

482

### 483 **YisK possesses at least one additional target**

484           Although YisK expression in a  $\Delta ponA \Delta mbl$  mutant did not result in cell-widening, we  
485 observed that the induced cells appeared qualitatively shorter than the uninduced control,  
486 suggesting that YisK might possess a second activity (Fig 6B). Quantitation of cell lengths in a  
487  $\Delta ponA \Delta mbl$  mutant following YisK expression revealed that the YisK-induced cells were ~20%  
488 shorter than the uninduced cells (Fig 7A). In contrast, YodL expression did not result in a change  
489 in cell length in a  $\Delta ponA \Delta mreB$  mutant (Fig 7B), suggesting the the cell shortening effect is  
490 specific to YisK. We hypothesized that MreBH, the third and final *B. subtilis* MreB family  
491 member, might be YisK's additional target. We hypothesized that if MreBH is the additional  
492 target, then the cell shortening observed upon YisK expression in a  $\Delta ponA \Delta mbl$  mutant strain  
493 should be lost in a  $\Delta ponA \Delta mbl \Delta mreBH$  mutant background. However, we found that even  
494 when *mreBH* was additionally deleted, YisK expression still resulted in cell shortening (Fig 7C).  
495 We conclude that YisK likely has at least one additional target that is not MreB or Mbl  
496 dependent, and that this additional target regulates some aspect of cell length.

497

## 498 **Discussion**

### 499 *YodL and YisK's functional targets*

500           Misexpression of YodL during vegetative growth results in cell-widening and lysis, and  
501 spontaneous suppressor mutations conferring resistance to YodL occur primarily in *mreB*. MreB  
502 is also required for YodL's cell-widening activity, whereas Mbl is not. By comparison,  
503 expression of YisK during vegetative growth also results in cell-widening and lysis, however,  
504 spontaneous suppressor mutations conferring resistance to YisK occur primarily in *mbl*. YisK's  
505 cell-widening activity requires Mbl, but not MreB. The simplest interpretation of these results is

506 that YodL targets MreB function, while YisK targets Mbl function. Alternatively, YodL and  
507 YisK could target other factors that affect cell shape and simply require MreB and Mbl for their  
508 respective functions.

509 MreB variants specifically resistant to YodL activity, MreB<sub>N145D</sub>, MreB<sub>P147R</sub> and  
510 MreB<sub>R282S</sub>, all result in charge change substitutions in residues previously shown to constitute the  
511 RodZ-MreB interaction surface (equivalent *T. maritima* residues are: MreB<sub>N140</sub>, MreB<sub>N142</sub> and  
512 MreB<sub>R279</sub>)(18). MreB<sub>G143A</sub>, which exhibits cross-resistance to YisK, also maps near the RodZ-  
513 MreB interaction interface. The two remaining YodL-resistant MreB variants occur in  
514 (MreB<sub>R117G</sub>) or near (MreB<sub>G323E</sub>) residues previously associated with bypass of RodZ essentiality  
515 in *E. coli* (Fig S5)(25). A simple model explaining both the nature of the MreB variants we  
516 obtained in the suppressor selections, and YodL's MreB-dependent effect on cell shape, is that  
517 YodL acts by disrupting the interaction between RodZ and MreB. In this model, MreB's RodZ-  
518 independent activities would remain functional, and several observations are consistent with this  
519 idea. If YodL were to completely inactivate MreB function, then we would expect that  
520 expressing YodL in a  $\Delta ponA \Delta mbl \Delta mreBH$  background would generate round cells, similar to  
521 the phenotype observed when MreB is depleted in a  $\Delta mbl \Delta mreBH$  mutant background (31), or  
522 when *mreB*, *mbl*, and *mreBH* are deleted in backgrounds with upregulated *sigI* expression (the  
523 triple mutant is otherwise lethal)(30). However, we observe that cells expressing YodL in a  
524  $\Delta ponA \Delta mbl \Delta mreBH$  mutant instead form wide rods (Fig 6A). If YodL does specifically target  
525 MreB activity, then these results suggest that MreB likely retains at least some of its width-  
526 maintenance function. Morgenstein et al. recently found that the interaction between RodZ and  
527 MreB in *E. coli* is required for MreB rotation, but that MreB rotation was not required for rod

528 shape or cell viability under standard laboratory conditions (26). This study is consistent with  
529 prior findings indicating that RodZ is not absolutely required for maintenance of rod shape (25).

530 We hypothesize that the substitutions obtained in residues near the RodZ-MreB interface  
531 either enhance RodZ-MreB interaction, or decrease the ability of YodL to disrupt the RodZ-  
532 MreB interface. Although we did not identify YodL-resistant suppressor mutations in *rodZ*, it is  
533 possible that the requisite *rodZ* mutations are rare or lethal for the cell, thus we cannot rule out  
534 the possibility that YodL could target RodZ function. Similarly, although we found that MreB is  
535 required for YodL activity, we can envision a scenario in which a YodL-MreB interaction may  
536 be necessary to localize YodL to a cellular location where it can be effective against RodZ or  
537 some other cellular component. We think this possibility is less likely, as cells expressing YodL  
538 have a distinct phenotype from RodZ depletion in *B. subtilis*. More specifically, YodL  
539 expression results in cell widening and tapered poles (Fig 1B), whereas RodZ-depleted cells  
540 generate wide rods (22), similar to the phenotype we observed following YodL expression in a  
541  $\Delta_{ponA} \Delta_{mbl} \Delta_{mreBH}$  mutant (Fig 6A). These results argue against the idea that YodL could  
542 work by inactivating RodZ function completely. Future work aimed at characterizing the nature  
543 of the YodL resistant suppressors and the effect of YodL on MreB function will shed light on the  
544 mechanism underlying YodL's observed activity.

545 Only three Mbl variants, Mbl<sub>R63C</sub>, Mbl<sub>ΔS251</sub>, and Mbl<sub>P309L</sub>, showed specificity in  
546 resistance to YisK over YodL. Mbl<sub>R63C</sub>, Mbl<sub>D153N</sub>, Mbl<sub>G156D</sub>, Mbl<sub>T158A</sub>, Mbl<sub>E204G</sub>, Mbl<sub>P309L</sub> and  
547 Mbl<sub>A314T</sub> occur in residues that form Mbl's predicted ATP-binding pocket (Fig S6), and  
548 substitutions in all seven of these residues have been previously implicated in A22 resistance  
549 (Fig S6)(12, 64, 65). We speculate that most, if not all of the substitutions in Mbl's ATP-binding  
550 pocket are gain-of-function with respect to Mbl polymerization, a hypothesis that can ultimately



551 be tested in vitro. Similarly, we hypothesize that the Mbl<sub>M511</sub> substitution, located at the MreB  
552 head-tail polymerization interface (63), may overcome YisK activity by promoting Mbl  
553 polymerization. MreB<sub>E262</sub> of *C. crescentus*, equivalent to *B. subtilis* Mbl<sub>E250</sub> (Fig S6), is located  
554 at the interaction interface of antiparallel MreB protofilament bundles (68). If *B. subtilis* Mbl<sub>E250</sub>  
555 is also present at this interface (this has not been tested to our knowledge), then Mbl<sub>E250K</sub> could  
556 promote resistance to YodL and YisK by enhancing Mbl bundling. How might YisK exert its  
557 activity? One idea is that YisK disrupts Mbl bundling, possibly by competing for sites required  
558 for protofilament formation. An alternative possibility is that YisK somehow prevents Mbl from  
559 effectively binding or hydrolyzing ATP. It is also possible that Mbl is simply required for YisK  
560 to target one or more other factors involved in cell-width control.

561 In addition to Mbl-dependent cell widening, YisK expression resulted in cell shortening,  
562 an effect that only became apparent in a  $\Delta ponA \Delta mbl$  mutant background (Fig 6B and 7A).  
563 Given the similarities of MreB, Mbl, and MreBH to each other, we initially hypothesized that  
564 YisK-dependent effects on MreB and/or MreBH might be responsible for the decrease in cell  
565 length we observed; however, we found that *mreBH* was not required for cell shortening (Fig 6B  
566 and Fig 7C). Since YisK expression results in a dramatic loss of cell shape in  $\Delta mreB$  mutant  
567 backgrounds (Fig 6A), we were unable to confidently assess cell length changes to determine if  
568 there is a requirement for MreB in the cell-shortening phenotype. It is unlikely that YisK's  
569 additional activity affects MreB's role in maintaining cell width (at least not without Mbl), as  
570 YisK-expressing cells retain rod shape when *mbl* and *mreBH* are both deleted (Fig 6B). An  
571 exciting alternative possibility is that YisK activity affects another factor involved in cell length  
572 control. One attractive candidate is the cell wall hydrolase CwlO, a known modulator of cell  
573 length in *B. subtilis* (69) which recent genetic data also suggests depends at least in part on Mbl

574 (35). Future experiments aimed at determining the identity and function of YisK's additional  
575 target should shed light on how cells regulate both cell length and cell width.

576

577 *Identification of genes involved in cellular organization through a novel gene*  
578 *discovery pipeline*

579

580 To systematically identify and characterize novel genes involved in cellular organization,  
581 we developed a gene discovery pipeline that combines known regulatory information (48),  
582 phenotypes obtained from misexpression screening, and suppressor selection analysis. The  
583 ability to identify genetic targets associated with the unknown genes provides a key parameter  
584 beyond phenotype from which to formulate testable hypotheses regarding each gene's possible  
585 function. The misexpression constructs we generated are inducible and present in single copy on  
586 the chromosome. We have found that to obtain phenotypes, our strategy works best when the  
587 unknown genes are expressed outside of their native regulatory context. Thus far, we have  
588 restricted our gene function discovery pipeline to *B. subtilis*; however, the general approach  
589 should be broadly applicable to other organisms and diverse screening strategies.

590

591 In this work, we describe the use of the pipeline to identify and characterize two *B.*  
592 *subtilis* genes, *yodL* and *yisK*, that produce proteins capable of targeting activities intrinsic to cell  
593 width control. Although *yodL* and *yisK* were not previously recognized as members of the  
594 Spo0A regulon, both genes have putative Spo0A boxes and possess promoters that exhibit  
595 expression patterns consistent with other Spo0A-regulated genes (Fig 2-4). YisK is also a  
596 member of the SigH regulon (50), and our expression analysis is also consistent with expression  
597 of *yisK* during stationary phase (Fig 3). If the putative Spo0A box we identified is utilized in  
598 vivo, then we would predict based on our expression profiling that *yisK* is transcribed during  
exponential and early stationary phase via SigH, and then repressed as Spo0A-P accumulates

599 during early sporulation. Such a pattern is similar to the regulation that has been proposed for  
600 *kinA* (56, 61). We also observe expression from  $P_{yodL}$  and  $P_{yisK}$  is reduced in the absence of  
601 Spo0A and SigH (Fig 3D-E). The specific contributions of these global regulators to *yodL* and  
602 *yisK* regulation cannot be determined by analyzing the expression profiles of the *sigH* and *spo0A*  
603 deletion strains alone, since *spo0A* depends on SigH for upregulation during the early stages of  
604 sporulation (53, 56). Moreover, since Spo0A inhibits expression of the *sigH* repressor AbrB (70-  
605 73), a *spo0A* mutant is also down for *sigH* expression.

606         A  $\Delta yodL \Delta yisK$  double mutant reproducibly produces ~20% less heat-stable spores than  
607 wildtype, suggesting that the YodL and YisK have functions that affect spore development  
608 (either directly or indirectly). Most studies on sporulation genes are biased toward factors that  
609 reduce sporulation efficiency by an order of magnitude or more in a standard heat-kill assay.  
610 However, even small differences in fitness (if reproducible) can contribute significantly to the  
611 ability of an organism to persist, especially in competitive environments (74). The 20%  
612 reduction in heat-resistant spores we observe in cells lacking YisK and YodL would likely result  
613 in a substantial fitness disadvantage to cells in the environment. We do not currently understand  
614 how YodL and YisK might function in spore development, but the identification of MreB and  
615 Mbl as genetic targets suggests the proteins likely regulate some aspect of PG synthesis. Future  
616 studies will be aimed at understanding the molecular and biochemical basis of YodL and YisK  
617 activity.

618         In this study, the morphological phenotypes associated with YodL and YisK occurred  
619 when the genes were expressed during vegetative growth. Consequently, it is formally possible  
620 (although we think unlikely), that the targeting of MreB and Mbl is simply a coincidence that is  
621 unrelated to the potential functions of the proteins during stationary phase or sporulation.

622 Regardless of what YodL and YisK's physiological roles turn out to be, we have already been  
623 able to utilize misexpression of the proteins to obtain interesting variants of both MreB and Mbl  
624 that can now be used to generate testable predictions regarding how MreB and Mbl function in  
625 *B. subtilis*. Moreover, the apparent specificity with which YodL and YisK appear to target MreB  
626 and Mbl, respectively, make them potentially powerful tools to differentially target the activities  
627 of these two highly similar paralogs in vivo. Of course, more studies will be required to  
628 determine if YodL and YisK interact directly or indirectly to modulate MreB and Mbl activity.  
629 In the meantime, it is exciting to speculate that many undiscovered modulators of MreB and  
630 MreB-like proteins exist, and that we have only just begun to scratch the surface regarding  
631 regulation of this important class of proteins. The identification and characterization of such  
632 modulators could go a long way toward addressing the significant gaps in our knowledge that  
633 exist regarding the regulation of PG synthesis in bacteria.

634

## 635 **Acknowledgments**

636 We thank members of the Herman Lab for critical reading of the manuscript, Benjamin Mercado  
637 for help with the whole-genome sequencing analysis, and Allyssa Miller, Benjamin Mercado,  
638 Jared McAnulty, and Simon Rousseau for their efforts toward generating and screening the  
639 BEIGEL.

641

642

643

644

645

646

647

648

649

650

651  
652  
653  
654  
655  
656  
657  
658  
659

Table 1

Strain	Strain #	Total cfu	Heat-resistant cfu	Sporulation efficiency	Relative sporulation efficiency
wildtype	<i>B. subtilis</i> 168	$2.8 \times 10^8$ ( $\pm 4.7 \times 10^7$ )	$1.9 \times 10^8$ ( $\pm 4.5 \times 10^7$ )	66.9% ( $\pm 5$ )	100% <sup>663</sup> 664
$\Delta yodL$	BYD276	$2.6 \times 10^8$ ( $\pm 3.9 \times 10^7$ )	$1.7 \times 10^8$ ( $\pm 2.8 \times 10^7$ )	65.2% ( $\pm 7$ )	97% <sup>665</sup> 666
$\Delta yisK$	BYD278	$2.7 \times 10^8$ ( $\pm 4.6 \times 10^7$ )	$2.4 \times 10^8$ ( $\pm 2.7 \times 10^7$ )	63.1% ( $\pm 6$ )	94% <sup>667</sup> 668
$\Delta yodL \Delta yisK$	BYD279	$3.1 \times 10^8$ ( $\pm 6.5 \times 10^7$ )	$1.7 \times 10^8$ ( $\pm 4.1 \times 10^7$ )	54.1% ( $\pm 4$ )	81% <sup>669</sup> 670
$\Delta yodL \Delta yisK$ <i>P<sub>yisK</sub>-yisK</i>	BYD510	$3.4 \times 10^8$ ( $\pm 3.3 \times 10^7$ )	$2.3 \times 10^8$ ( $\pm 4.1 \times 10^7$ )	66.2% ( $\pm 7$ )	99% <sup>671</sup> 672 673 674

675 **Table 1. Sporulation efficiency of *yodL* and *yisK* mutants.** Sporulation efficiency is the  
676 number of spores/ml divided by the total cfu/ml  $\times$  100%. Relative sporulation efficiency is  
677 sporulation efficiency normalized to wildtype  $\times$  100%. The data shown is the average of six  
678 independent biological replicates. The difference in sporulation efficiency between wildtype  
679 and the  $\Delta yodL \Delta yisK$  double mutant is statistically significant ( $P < 0.0006$ ).

680  
681  
682  
683  
684  
685  
686  
687  
688  
689  
690  
691

692  
693  
694  
695  
696  
697  
698  
699  
700

Table 2

Variants obtained following YodL misexpression			
<i>mreB</i>	MreB Variants	+YodL	+YisK
CGC→GGC	R117G <sup>1</sup>	R	R
GGA→GCA	G143A	R	R
AAT→GAT*	<u>N145D</u> <sup>2</sup>	R	S
CCA→CGA*	<u>P147R</u> <sup>1,2</sup>	R	S
AGC→AGA	<u>S154R</u> <sup>1,2</sup>	--	--
AGC→AGA	S154R <sup>1</sup>	R	R
CGC→TGC	R230C		
AGA→AGT*	<u>R282S</u> <sup>1,2</sup>	R	S
GGG→GAG	G323E <sup>1</sup>	R	R
<i>mbl</i>	Mbl Variants	+YodL	+YisK
ACG→ATG	T158M	R	R
GAA→AAA*	E250K <sup>1</sup>	R	R
ACA→ATA	T317I	R	R
Variants obtained following YisK misexpression			
<i>mreB</i>	MreB Variants	+YisK	+YodL
CGC→TGC	R117G	R	R
<i>mbl</i>	Mbl Variants	+YisK	+YodL
ATG→ATA	M51I <sup>3</sup>	R	R
CGC→TGC	<u>R63C</u> <sup>3</sup>	R	S
GAC→AAC*	D153N <sup>3</sup>	R	R
GGC→GAC	G156D <sup>3</sup>	R	R
ACG→GCG*	T158A <sup>3</sup>	R	R
GAG→GGG	E204G <sup>3</sup>	R	R
GAA→AAA	E250K	R	R
TCT→ $\Delta\Delta\Delta$	<u><math>\Delta</math>S251</u>	R	S
CCT→CTT	<u>P309L</u> <sup>3</sup>	R	S
GCC→ACC	A314T <sup>3</sup>	R	R

701

702 **Table 2. Analysis of suppressor strains resistant to YodL and/or YisK.**

703 The suppressor selections are described in detail in materials and methods. Candidate mutations  
704 were introduced into clean genetic backgrounds harboring three copies of  $P_{hy}$ -*yodL* or three  
705 copies of  $P_{hy}$ -*yisK*, and the resultant strains were assessed for resistance (R) or sensitivity (S) to  
706 either *yodL* or *yisK* expression as judged by ability to grow on LB plates supplemented with 1

707 mM IPTG and 100  $\mu$ g/ml spectinomycin. <sup>1</sup>Originally identified using whole-genome sequencing  
708 (Table S1). <sup>2</sup>Residues previously implicated in the RodZ-MreB interaction (18). <sup>3</sup>Residues  
709 previously implicated in resistance to A22 (64, 65, 75). The (\*) indicates that two suppressors  
710 possessing the same nucleotide change were obtained in original selection. The underlined  
711 residues displayed specificity in resistance to YodL over YisK (top) or YisK over YodL  
712 (bottom).

713

## 714 **Figure Legends**

715

716 **Figure 1. Misexpression of YodL and YisK prevents cell growth on solid media and causes**  
717 **loss of cell shape in liquid media.**

718 (A) Cells harboring one (1X) or two (2X) copies of  $P_{hy}$ -*yodL* (BAS040 and BAS191) or  $P_{hy}$ -*yisK*  
719 (BAS041 and BYD074)(B) were streaked on an LB plate supplemented with 100  $\mu$ g/ml  
720 spectinomycin and, when indicated, 1 mM IPTG or 1 mM IPTG and the denoted concentration  
721 of  $MgCl_2$ . Plates were incubated for ~16 hrs at 37°C before image capture (top). (B) The strains  
722 described above were grown in LB-Lennox media at 37°C to mid-exponential and back-diluted  
723 to an  $OD_{600}$  of ~0.02. When indicated, 1 mM IPTG or 1 mM IPTG and the denoted  
724 concentration of  $MgCl_2$  was added. Cells were grown for 1.5 hrs at 37°C before image capture.  
725 Membranes were stained with TMA-DPH. All images were scaled identically.

726

727 **Figure 2. DNA sequence upstream of *yodL* and *yisK*.**

728 (A) Putative Spo0A box (underlined) upstream of the *yodL* start codon. (B) SigH binding motifs  
729 (double underline) and putative Spo0A box (underlined) upstream of *yisK* start codon.

730

731 **Figure 3. Expression from *yodL* and *yisK* promoters during a CH timecourse.**

732 Expression from the putative *yodL* and *yisK* promoter regions was monitored in CH medium at  
733 37°C over a timecourse. The OD<sub>600</sub> (A and B) and production of either GFP (C) or beta-  
734 galactosidase (D and E) was monitored at 30 min intervals. Membranes were stained with TMA-  
735 DPH. All GFP channel images were captured with 1 sec exposures and scaled identically to  
736 allow for direct comparison. In this media, time 0 represents the last exponential timepoint, not  
737 the initiation of sporulation.

738

739 **Figure 4. Expression from *yodL* and *yisK* promoters following sporulation by**

740 **resuspension.** Expression from the putative *yodL* and *yisK* promoter regions was monitored in  
741 resuspension medium. The production of either GFP (A) or beta-galactosidase (B and C) was  
742 monitored at 20 min intervals. Membranes were stained with TMA-DPH. All GFP channel  
743 images were captured with 1 sec exposures and scaled identically to allow for direct  
744 comparison.

745

746 **Figure 5. YodL and YisK co-misexpression causes cell lysis.**

747 (A) BYD361 ( $P_{hy}$ -*yodL*,  $P_{hy}$ -*yisK*) and BYD281 (2X  $P_{hy}$ -*yodL*, 2X  $P_{hy}$ -*yisK*) were streaked on an  
748 LB plate with 100 µg/ml spectinomycin and, when indicated 1 mM IPTG or 1 mM IPTG and  
749 the denoted concentration of MgCl<sub>2</sub>. (B) Cells were grown in LB-Lennox media at 37°C to mid-  
750 exponential and back-diluted to an OD<sub>600</sub> of ~0.02. When indicated 1 mM IPTG or 1 mM IPTG  
751 and the denoted concentration of MgCl<sub>2</sub> were added. Cells were then grown for 1.5 hrs at 37°C



752 before image capture. Membranes are stained with TMA-DPH. All images are shown at the  
753 same magnification.

754

755 **Figure 6. YodL and YisK's cell-widening activities require MreB and Mbl, respectively.**

756 (A) Cells harboring 2X copies of  $P_{hy}$ -*yodL* in a wildtype (BAS191),  $\Delta$ *ponA* (BYD176),  $\Delta$ *ponA*  
757  $\Delta$ *mreB* (BYD263),  $\Delta$ *ponA*  $\Delta$ *mbl* (BYD259) or  $\Delta$ *ponA*  $\Delta$ *mbl*  $\Delta$ *mreBH* (BAS249) background  
758 were grown at 37°C in LB supplemented with 10 mM MgCl<sub>2</sub> to mid-exponential. To induce  
759 *yodL* expression, cells were back-diluted to an OD<sub>600</sub> of ~0.02 in LB with 10 mM MgCl<sub>2</sub>, and  
760 IPTG (1 mM) was added. Cells were grown for 1.5 hrs at 37°C before image capture.

761 Membranes are stained with TMA-DPH. All images are shown at the same magnification. (B)

762 Cells harboring 2X copies of  $P_{hy}$ -*yisK* in a wildtype (BYD074),  $\Delta$ *ponA* (BYD175),  $\Delta$ *ponA*  
763  $\Delta$ *mreB* (BYD262),  $\Delta$ *ponA*  $\Delta$ *mbl* (BYD258) or  $\Delta$ *ponA*  $\Delta$ *mbl*  $\Delta$ *mreBH* (BAS248) background  
764 were grown at 37°C in LB supplemented with 10 mM MgCl<sub>2</sub> to mid-exponential. To induce  
765 *yisK* expression, cells were back-diluted to an OD<sub>600</sub> of ~0.02 in LB with 10 mM MgCl<sub>2</sub>, and  
766 IPTG (1 mM) was added. Cells were grown for 1.5 hrs at 37°C before image capture.

767 Membranes are stained with TMA-DPH. All images are shown at the same magnification.

768

769 **Figure 7. YisK expression results in cell shortening.**

770 (A) Cells harboring 2X copies of  $P_{hy}$ -*yisK* in a  $\Delta$ *ponA*  $\Delta$ *mbl* background (BYD262) were grown  
771 at 37°C in LB supplemented with 10 mM MgCl<sub>2</sub> to mid-exponential. To induce *yisK* expression,  
772 cells were back-diluted to an OD<sub>600</sub> of ~0.02 in LB with 10 mM MgCl<sub>2</sub> and IPTG (1 mM) was  
773 added. Cells were grown for 1.5 hrs at 37°C before image capture. Membranes are stained with  
774 TMA-DPH. Cell lengths (n=500/condition) were measured before and after *yisK* expression and

775 rank-ordered from smallest to largest along the x-axis so the entire population could be  
776 visualized without binning. The uninduced population (black) is juxtaposed behind the induced  
777 population (semi-transparent, gray). The difference in average cell length before and after  $P_{hy}$ -  
778 *ysisK* induction were statistically significant ( $P<0.0001$ ). (B) Cells harboring 2X copies of  $P_{hy}$ -  
779 *yodL* in a  $\Delta ponA \Delta mreB$  background (BYD263) were grown, quantitated, and plotted as  
780 described above. The difference in average cell length before and after  $P_{hy}$ -*yodL* induction were  
781 not statistically significant. (C) Cells harboring 2X copies of  $P_{hy}$ -*ysisK* in a  $\Delta ponA \Delta mbl \Delta mreBH$   
782 background (BAS248) were grown, quantitated, and plotted as described above. The difference  
783 in average cell length before and after  $P_{hy}$ -*ysisK* induction were statistically significant  
784 ( $P<0.0001$ ).

785

## 786 References

787

- 788 1. **Young KD.** 2010. Bacterial shape: two-dimensional questions and possibilities.  
789 *Annu Rev Microbiol* **64**:223-240.
- 790 2. **Silhavy TJ, Kahne D, Walker S.** 2010. The bacterial cell envelope. *Cold Spring Harb*  
791 *Perspect Biol* **2**:a000414.
- 792 3. **Holtje JV.** 1998. Growth of the stress-bearing and shape-maintaining murein  
793 sacculus of *Escherichia coli*. *Microbiol Mol Biol Rev* **62**:181-203.
- 794 4. **Young KD.** 2007. Bacterial morphology: why have different shapes? *Curr Opin*  
795 *Microbiol* **10**:596-600.
- 796 5. **Young KD.** 2006. The selective value of bacterial shape. *Microbiol Mol Biol Rev*  
797 **70**:660-703.
- 798 6. **Randich AM, Brun YV.** 2015. Molecular mechanisms for the evolution of bacterial  
799 morphologies and growth modes. *Front Microbiol* **6**:580.
- 800 7. **Fenton AK, Gerdes K.** 2013. Direct interaction of FtsZ and MreB is required for  
801 septum synthesis and cell division in *Escherichia coli*. *EMBO J* **32**:1953-1965.
- 802 8. **Figge RM, Divakaruni AV, Gober JW.** 2004. MreB, the cell shape-determining  
803 bacterial actin homologue, co-ordinates cell wall morphogenesis in *Caulobacter*  
804 *crenscentus*. *Mol Microbiol* **51**:1321-1332.

- 805 9. **Ouellette SP, Karimova G, Subtil A, Ladant D.** 2012. *Chlamydia* co-opts the rod  
806 shape-determining proteins MreB and Pbp2 for cell division. *Mol Microbiol* **85**:164-  
807 178.
- 808 10. **Salje J, van den Ent F, de Boer P, Lowe J.** 2011. Direct membrane binding by  
809 bacterial actin MreB. *Mol Cell* **43**:478-487.
- 810 11. **Colavin A, Hsin J, Huang KC.** 2014. Effects of polymerization and nucleotide  
811 identity on the conformational dynamics of the bacterial actin homolog MreB. *Proc*  
812 *Natl Acad Sci U S A* **111**:3585-3590.
- 813 12. **Gitai Z, Dye NA, Reisenauer A, Wachi M, Shapiro L.** 2005. MreB actin-mediated  
814 segregation of a specific region of a bacterial chromosome. *Cell* **120**:329-341.
- 815 13. **Iwai N, Nagai K, Wachi M.** 2002. Novel S-benzylisothiourea compound that induces  
816 spherical cells in *Escherichia coli* probably by acting on a rod-shape-determining  
817 protein(s) other than penicillin-binding protein 2. *Biosci Biotechnol Biochem*  
818 **66**:2658-2662.
- 819 14. **Bean GJ, Flickinger ST, Westler WM, McCully ME, Sept D, Weibel DB, Amann KJ.**  
820 2009. A22 disrupts the bacterial actin cytoskeleton by directly binding and inducing  
821 a low-affinity state in MreB. *Biochemistry* **48**:4852-4857.
- 822 15. **Takacs CN, Poggio S, Charbon G, Pucheault M, Vollmer W, Jacobs-Wagner C.**  
823 2010. MreB drives de novo rod morphogenesis in *Caulobacter crescentus* via  
824 remodeling of the cell wall. *J Bacteriol* **192**:1671-1684.
- 825 16. **Kruse T, Bork-Jensen J, Gerdes K.** 2005. The morphogenetic MreBCD proteins of  
826 *Escherichia coli* form an essential membrane-bound complex. *Mol Microbiol* **55**:78-  
827 89.
- 828 17. **Bendezu FO, de Boer PA.** 2008. Conditional lethality, division defects, membrane  
829 involution, and endocytosis in *mre* and *mrd* shape mutants of *Escherichia coli*. *J*  
830 *Bacteriol* **190**:1792-1811.
- 831 18. **van den Ent F, Johnson CM, Persons L, de Boer P, Lowe J.** 2010. Bacterial actin  
832 MreB assembles in complex with cell shape protein RodZ. *EMBO J* **29**:1081-1090.
- 833 19. **Varma A, Young KD.** 2009. In *Escherichia coli*, MreB and FtsZ direct the synthesis of  
834 lateral cell wall via independent pathways that require PBP 2. *J Bacteriol* **191**:3526-  
835 3533.
- 836 20. **Kawai Y, Daniel RA, Errington J.** 2009. Regulation of cell wall morphogenesis in  
837 *Bacillus subtilis* by recruitment of PBP1 to the MreB helix. *Mol Microbiol* **71**:1131-  
838 1144.
- 839 21. **Bendezu FO, Hale CA, Bernhardt TG, de Boer PA.** 2009. RodZ (YfgA) is required  
840 for proper assembly of the MreB actin cytoskeleton and cell shape in *E. coli*. *EMBO J*  
841 **28**:193-204.
- 842 22. **Muchova K, Chromikova Z, Barak I.** 2013. Control of *Bacillus subtilis* cell shape by  
843 RodZ. *Environ Microbiol* **15**:3259-3271.
- 844 23. **Alyahya SA, Alexander R, Costa T, Henriques AO, Emonet T, Jacobs-Wagner C.**  
845 2009. RodZ, a component of the bacterial core morphogenic apparatus. *Proc Natl*  
846 *Acad Sci U S A* **106**:1239-1244.
- 847 24. **Niba ET, Li G, Aoki K, Kitakawa M.** 2010. Characterization of *rodZ* mutants: RodZ is  
848 not absolutely required for the cell shape and motility. *FEMS Microbiol Lett* **309**:35-  
849 42.

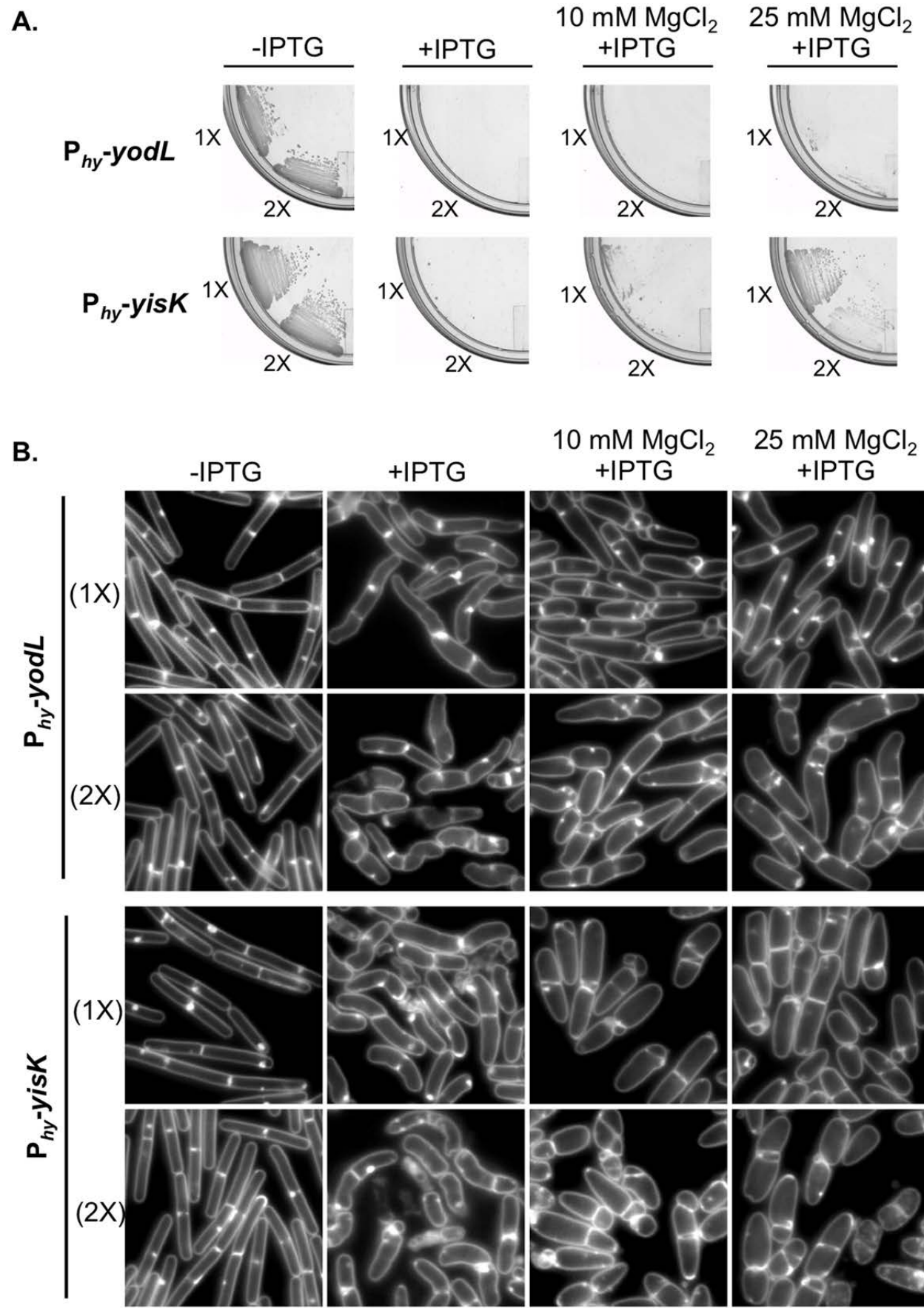
- 850 25. **Shiomi D, Toyoda A, Aizu T, Ejima F, Fujiyama A, Shini T, Kohara Y, Niki H.**  
851 2013. Mutations in cell elongation genes *mreB*, *mrdA* and *mrdB* suppress the shape  
852 defect of RodZ-deficient cells. *Mol Microbiol* **87**:1029-1044.
- 853 26. **Morgenstein RM, Bratton BP, Nguyen JP, Ouzounov N, Shaevitz JW, Gitai Z.**  
854 2015. RodZ links MreB to cell wall synthesis to mediate MreB rotation and robust  
855 morphogenesis. *Proc Natl Acad Sci U S A*.
- 856 27. **Cabeen MT, Jacobs-Wagner C.** 2010. The bacterial cytoskeleton. *Annu Rev Genet*  
857 **44**:365-392.
- 858 28. **Carballido-Lopez R, Formstone A, Li Y, Ehrlich SD, Noirot P, Errington J.** 2006.  
859 Actin homolog MreBH governs cell morphogenesis by localization of the cell wall  
860 hydrolase LytE. *Dev Cell* **11**:399-409.
- 861 29. **Formstone A, Errington J.** 2005. A magnesium-dependent *mreB* null mutant:  
862 implications for the role of *mreB* in *Bacillus subtilis*. *Mol Microbiol* **55**:1646-1657.
- 863 30. **Schirner K, Errington J.** 2009. The cell wall regulator  $\sigma^I$  specifically suppresses the  
864 lethal phenotype of *mbl* mutants in *Bacillus subtilis*. *J Bacteriol* **191**:1404-1413.
- 865 31. **Kawai Y, Asai K, Errington J.** 2009. Partial functional redundancy of MreB  
866 isoforms, MreB, Mbl and MreBH, in cell morphogenesis of *Bacillus subtilis*. *Mol*  
867 *Microbiol* **73**:719-731.
- 868 32. **Defeu Soufo HJ, Graumann PL.** 2006. Dynamic localization and interaction with  
869 other *Bacillus subtilis* actin-like proteins are important for the function of MreB. *Mol*  
870 *Microbiol* **62**:1340-1356.
- 871 33. **Mirouze N, Ferret C, Yao Z, Chastanet A, Carballido-Lopez R.** 2015. MreB-  
872 Dependent Inhibition of Cell Elongation during the Escape from Competence in  
873 *Bacillus subtilis*. *PLoS Genet* **11**:e1005299.
- 874 34. **Tseng CL, Shaw GC.** 2008. Genetic evidence for the actin homolog gene *mreBH* and  
875 the bacitracin resistance gene *bcrC* as targets of the alternative sigma factor *SigI* of  
876 *Bacillus subtilis*. *J Bacteriol* **190**:1561-1567.
- 877 35. **Dominguez-Cuevas P, Porcelli I, Daniel RA, Errington J.** 2013. Differentiated  
878 roles for MreB-actin isologues and autolytic enzymes in *Bacillus subtilis*  
879 morphogenesis. *Mol Microbiol* **89**:1084-1098.
- 880 36. **Masuda H, Tan Q, Awano N, Wu KP, Inouye M.** 2012. YeeU enhances the bundling  
881 of cytoskeletal polymers of MreB and FtsZ, antagonizing the CbtA (YeeV) toxicity in  
882 *Escherichia coli*. *Mol Microbiol* **84**:979-989.
- 883 37. **Tan Q, Awano N, Inouye M.** 2011. YeeV is an *Escherichia coli* toxin that inhibits cell  
884 division by targeting the cytoskeleton proteins, FtsZ and MreB. *Mol Microbiol*  
885 **79**:109-118.
- 886 38. **Masuda H, Tan Q, Awano N, Yamaguchi Y, Inouye M.** 2012. A novel membrane-  
887 bound toxin for cell division, CptA (YgfX), inhibits polymerization of cytoskeleton  
888 proteins, FtsZ and MreB, in *Escherichia coli*. *FEMS Microbiol Lett* **328**:174-181.
- 889 39. **Yakhnina AA, Gitai Z.** 2012. The small protein MbiA interacts with MreB and  
890 modulates cell shape in *Caulobacter crescentus*. *Mol Microbiol* **85**:1090-1104.
- 891 40. **Ababneh QO, Herman JK.** 2015. CodY regulates SigD levels and activity by binding  
892 to three sites in the *fla/che* Operon. *J Bacteriol* **197**:2999-3006.
- 893 41. **Harwood CR, Cutting SM.** 1990. Molecular biological methods for *Bacillus*. Wiley,  
894 New York, NY.

- 895 42. **Rasband W.** 1997-2015. ImageJ. U.S. National Institutes of Health, Bethesda,  
896 Maryland.
- 897 43. **Schaeffer P, Millet J, Aubert JP.** 1965. Catabolic repression of bacterial sporulation.  
898 Proc Natl Acad Sci U S A **54**:704-711.
- 899 44. **Harwood CRaC, S.M.** 1990. Molecular Biological Methods for Bacillus. Wiley, New  
900 York.
- 901 45. **Ababneh QO, Herman JK.** 2015. RelA inhibits Bacillus subtilis motility and  
902 chaining. J Bacteriol **197**:128-137.
- 903 46. **Abhayawardhane Y, Stewart GC.** 1995. *Bacillus subtilis* possesses a second  
904 determinant with extensive sequence similarity to the *Escherichia coli mreB*  
905 morphogene. J Bacteriol **177**:765-773.
- 906 47. **Leaver M, Errington J.** 2005. Roles for MreC and MreD proteins in helical growth of  
907 the cylindrical cell wall in *Bacillus subtilis*. Mol Microbiol **57**:1196-1209.
- 908 48. **Nicolas P, Mader U, Dervyn E, Rochat T, Leduc A, Pigeonneau N, Bidnenko E,  
909 Marchadier E, Hoebeke M, Aymerich S, Becher D, Bisicchia P, Botella E,  
910 Delumeau O, Doherty G, Denham EL, Fogg MJ, Fromion V, Goelzer A, Hansen A,  
911 Hartig E, Harwood CR, Homuth G, Jarmer H, Jules M, Klipp E, Le Chat L,  
912 Lecointe F, Lewis P, Liebermeister W, March A, Mars RA, Nannapaneni P,  
913 Noone D, Pohl S, Rinn B, Rugheimer F, Sappa PK, Samson F, Schaffer M,  
914 Schwikowski B, Steil L, Stulke J, Wiegert T, Devine KM, Wilkinson AJ, van Dijl  
915 JM, Hecker M, Volker U, Bessieres P, Noirot P.** 2012. Condition-dependent  
916 transcriptome reveals high-level regulatory architecture in *Bacillus subtilis*. Science  
917 **335**:1103-1106.
- 918 49. **Molle V, Fujita M, Jensen ST, Eichenberger P, Gonzalez-Pastor JE, Liu JS, Losick  
919 R.** 2003. The Spo0A regulon of *Bacillus subtilis*. Mol Microbiol **50**:1683-1701.
- 920 50. **Britton RA, Eichenberger P, Gonzalez-Pastor JE, Fawcett P, Monson R, Losick R,  
921 Grossman AD.** 2002. Genome-wide analysis of the stationary-phase sigma factor  
922 (sigma-H) regulon of *Bacillus subtilis*. J Bacteriol **184**:4881-4890.
- 923 51. **Arrieta-Ortiz ML, Hafemeister C, Bate AR, Chu T, Greenfield A, Shuster B, Barry  
924 SN, Gallitto M, Liu B, Kacmarczyk T, Santoriello F, Chen J, Rodrigues CD, Sato T,  
925 Rudner DZ, Driks A, Bonneau R, Eichenberger P.** 2015. An experimentally  
926 supported model of the *Bacillus subtilis* global transcriptional regulatory network.  
927 Mol Syst Biol **11**:839.
- 928 52. **Caspi R, Altman T, Billington R, Dreher K, Foerster H, Fulcher CA, Holland TA,  
929 Keseler IM, Kothari A, Kubo A, Krummenacker M, Latendresse M, Mueller LA,  
930 Ong Q, Paley S, Subhraveti P, Weaver DS, Weerasinghe D, Zhang P, Karp PD.**  
931 2014. The MetaCyc database of metabolic pathways and enzymes and the BioCyc  
932 collection of Pathway/Genome Databases. Nucleic Acids Res **42**:D459-471.
- 933 53. **Predich M, Nair G, Smith I.** 1992. *Bacillus subtilis* early sporulation genes *kinA*,  
934 *spo0F*, and *spo0A* are transcribed by the RNA polymerase containing sigma H. J  
935 Bacteriol **174**:2771-2778.
- 936 54. **Antoniewski C, Savelli B, Stragier P.** 1990. The spoIIJ gene, which regulates early  
937 developmental steps in Bacillus subtilis, belongs to a class of environmentally  
938 responsive genes. J Bacteriol **172**:86-93.
- 939 55. **Fujita M, Sadaie Y.** 1998. Promoter selectivity of the Bacillus subtilis RNA  
940 polymerase sigmaA and sigmaH holoenzymes. J Biochem **124**:89-97.

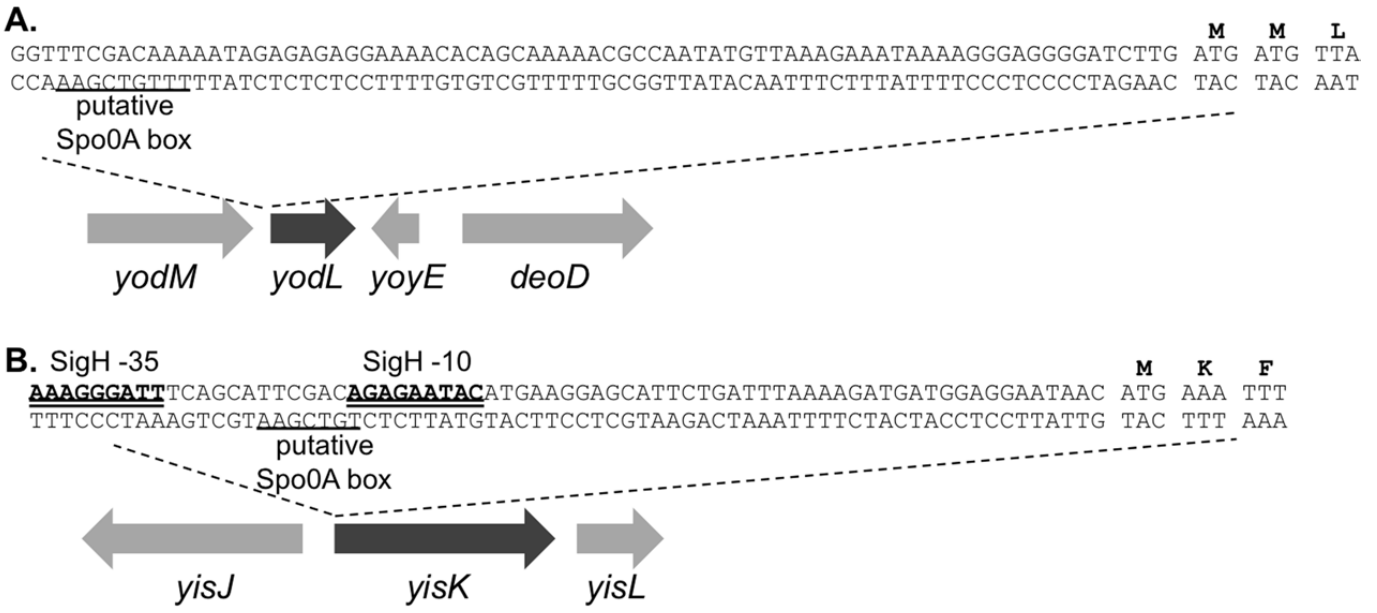


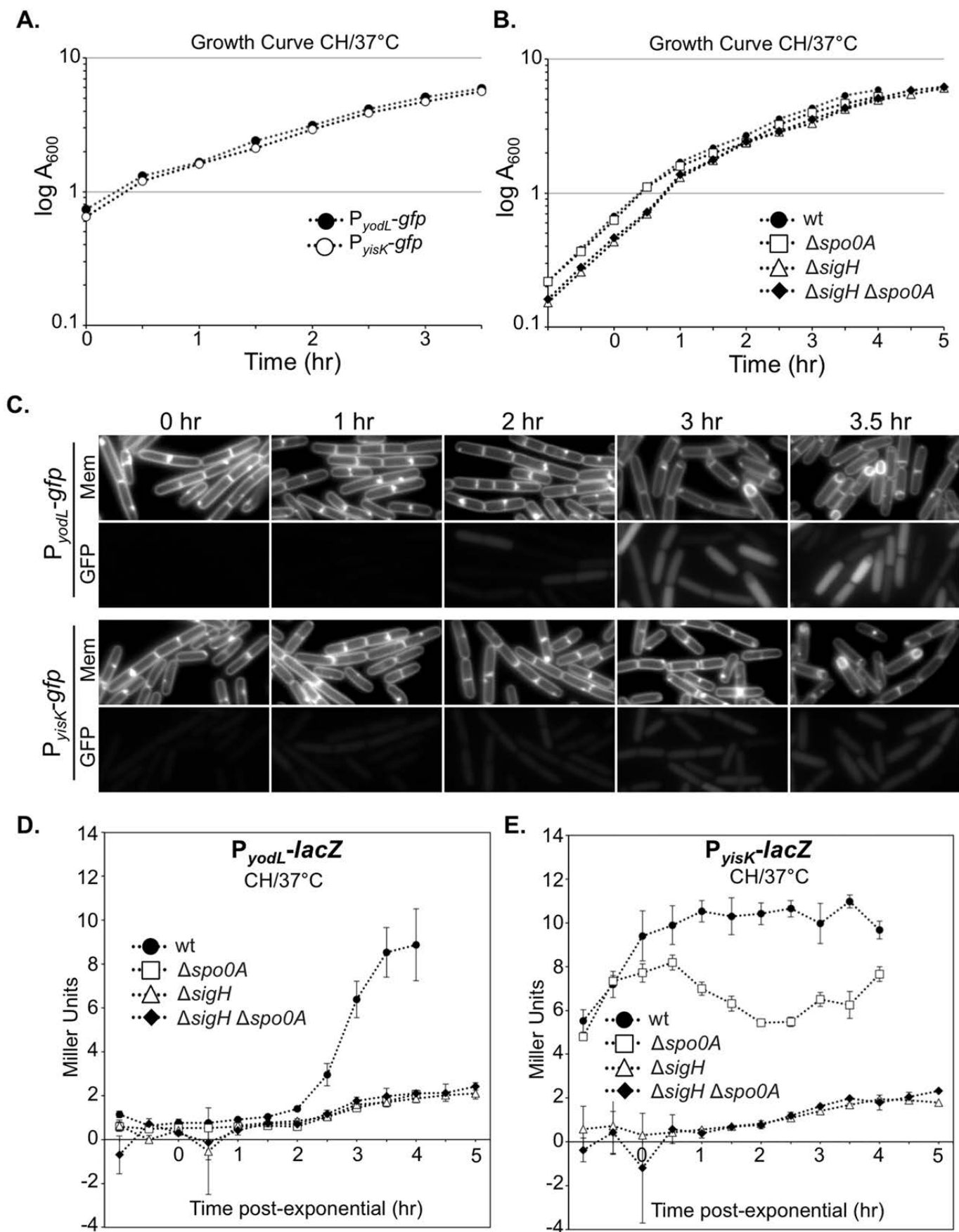
- 941 56. **Fujita M, Sadaie Y.** 1998. Feedback loops involving Spo0A and AbrB in in vitro  
942 transcription of the genes involved in the initiation of sporulation in *Bacillus*  
943 *subtilis*. *J Biochem* **124**:98-104.
- 944 57. **Chastanet A, Vitkup D, Yuan GC, Norman TM, Liu JS, Losick RM.** 2010. Broadly  
945 heterogeneous activation of the master regulator for sporulation in *Bacillus subtilis*.  
946 *Proc Natl Acad Sci U S A* **107**:8486-8491.
- 947 58. **de Jong IG, Veening JW, Kuipers OP.** 2010. Heterochronic phosphorelay gene  
948 expression as a source of heterogeneity in *Bacillus subtilis* spore formation. *J*  
949 *Bacteriol* **192**:2053-2067.
- 950 59. **Sterlini JM, Mandelstam J.** 1969. Commitment to sporulation in *Bacillus subtilis*  
951 and its relationship to development of actinomycin resistance. *Biochem J* **113**:29-37.
- 952 60. **Pan Q, Losick R.** 2003. Unique degradation signal for ClpCP in *Bacillus subtilis*. *J*  
953 *Bacteriol* **185**:5275-5278.
- 954 61. **Fujita M, Gonzalez-Pastor JE, Losick R.** 2005. High- and low-threshold genes in the  
955 Spo0A regulon of *Bacillus subtilis*. *J Bacteriol* **187**:1357-1368.
- 956 62. **Jiang M, Shao W, Perego M, Hoch JA.** 2000. Multiple histidine kinases regulate  
957 entry into stationary phase and sporulation in *Bacillus subtilis*. *Mol Microbiol*  
958 **38**:535-542.
- 959 63. **van den Ent F, Amos LA, Lowe J.** 2001. Prokaryotic origin of the actin cytoskeleton.  
960 *Nature* **413**:39-44.
- 961 64. **Dye NA, Pincus Z, Fisher IC, Shapiro L, Theriot JA.** 2011. Mutations in the  
962 nucleotide binding pocket of MreB can alter cell curvature and polar morphology in  
963 *Caulobacter*. *Mol Microbiol* **81**:368-394.
- 964 65. **Srivastava P, Demarre G, Karpova TS, McNally J, Chatteraj DK.** 2007. Changes in  
965 nucleoid morphology and origin localization upon inhibition or alteration of the  
966 actin homolog, MreB, of *Vibrio cholerae*. *J Bacteriol* **189**:7450-7463.
- 967 66. **Murray T, Popham DL, Setlow P.** 1998. *Bacillus subtilis* cells lacking penicillin-  
968 binding protein 1 require increased levels of divalent cations for growth. *J Bacteriol*  
969 **180**:4555-4563.
- 970 67. **Popham DL, Setlow P.** 1996. Phenotypes of *Bacillus subtilis* mutants lacking  
971 multiple class A high-molecular-weight penicillin-binding proteins. *J Bacteriol*  
972 **178**:2079-2085.
- 973 68. **van den Ent F, Izore T, Bharat TA, Johnson CM, Lowe J.** 2014. Bacterial actin  
974 MreB forms antiparallel double filaments. *Elife* **3**:e02634.
- 975 69. **Meisner J, Montero Llopis P, Sham LT, Garner E, Bernhardt TG, Rudner DZ.**  
976 2013. FtsEX is required for CwlO peptidoglycan hydrolase activity during cell wall  
977 elongation in *Bacillus subtilis*. *Mol Microbiol* **89**:1069-1083.
- 978 70. **Dubnau EJ, Cabane K, Smith I.** 1987. Regulation of spo0H, an early sporulation  
979 gene in bacilli. *J Bacteriol* **169**:1182-1191.
- 980 71. **Weir J, Predich M, Dubnau E, Nair G, Smith I.** 1991. Regulation of spo0H, a gene  
981 coding for the *Bacillus subtilis* sigma H factor. *J Bacteriol* **173**:521-529.
- 982 72. **Perego M, Spiegelman GB, Hoch JA.** 1988. Structure of the gene for the transition  
983 state regulator, abrB: regulator synthesis is controlled by the spo0A sporulation  
984 gene in *Bacillus subtilis*. *Mol Microbiol* **2**:689-699.
- 985 73. **Strauch M, Webb V, Spiegelman G, Hoch JA.** 1990. The Spo0A protein of *Bacillus*  
986 *subtilis* is a repressor of the abrB gene. *Proc Natl Acad Sci U S A* **87**:1801-1805.

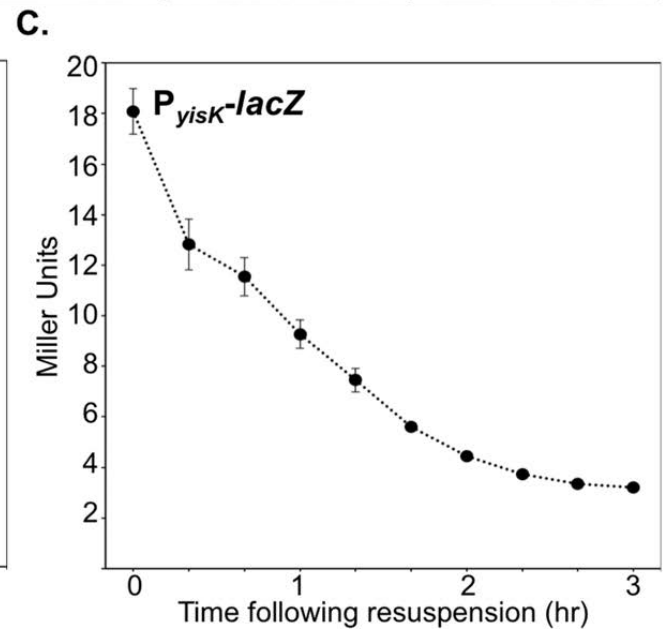
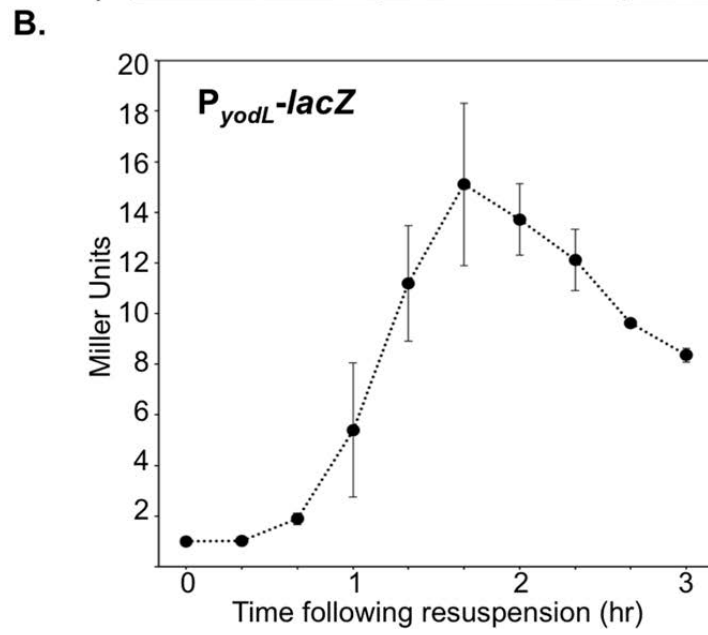
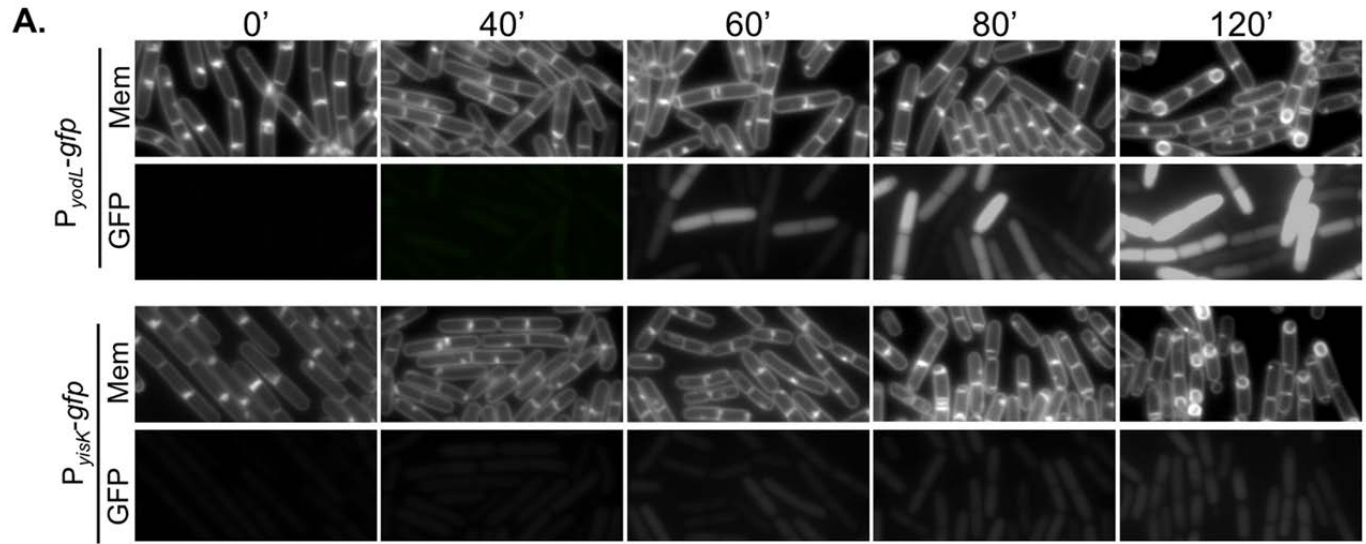
- 987 74. **Wiser MJ, Lenski RE.** 2015. A Comparison of Methods to Measure Fitness in  
988 *Escherichia coli*. PLoS One **10**:e0126210.  
989 75. **Gitai Z, Dye N, Shapiro L.** 2004. An actin-like gene can determine cell polarity in  
990 bacteria. Proc Natl Acad Sci U S A.  
991



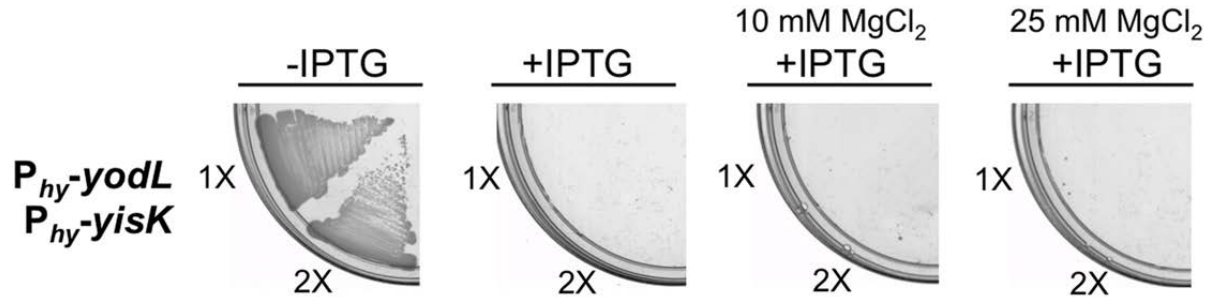




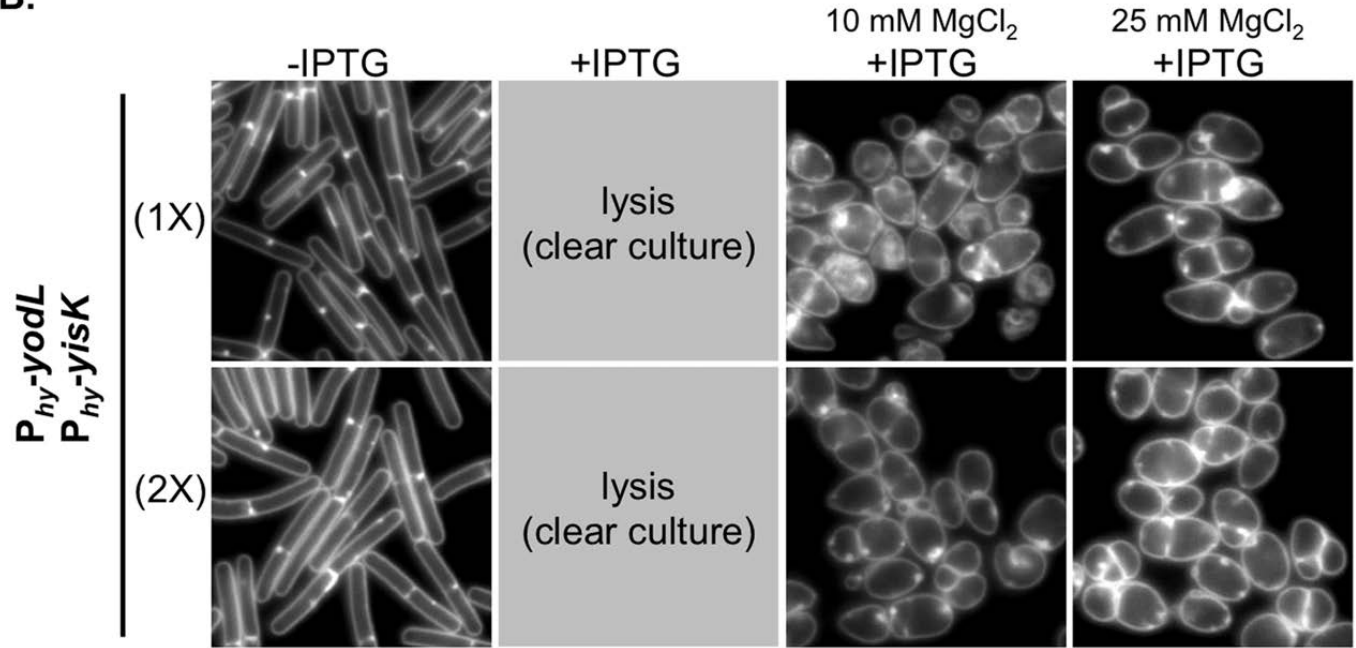




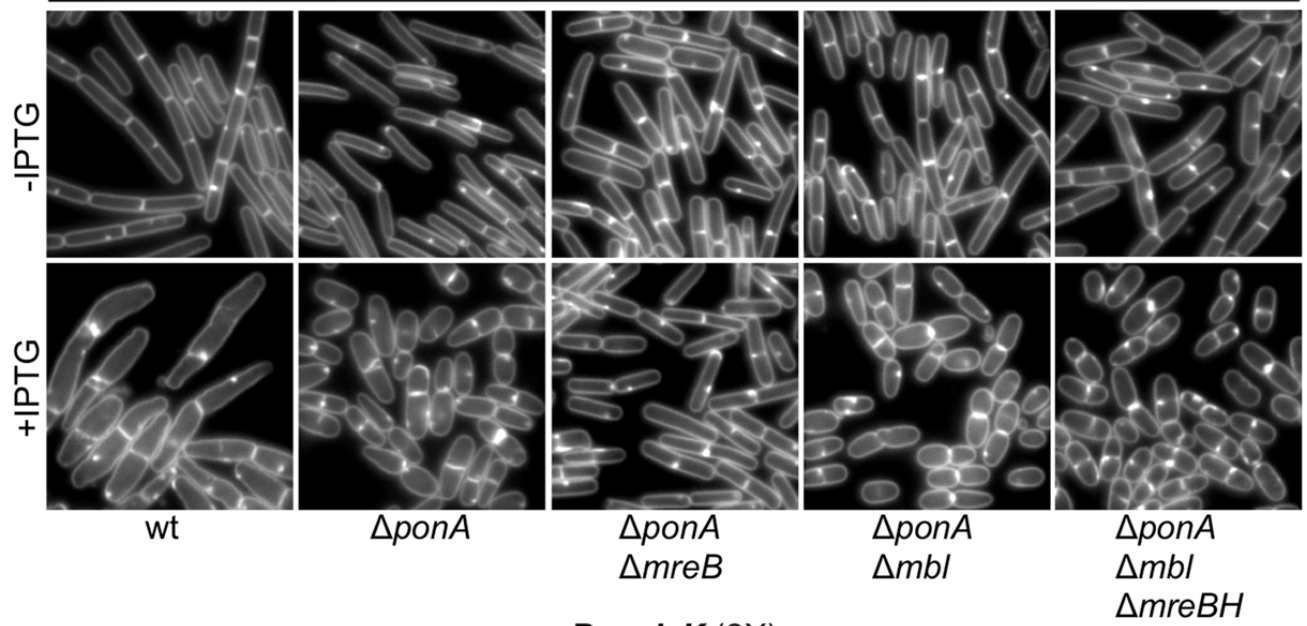
A.



B.



A.

 $P_{hy}$ -yodL (2X)

B.

 $P_{hy}$ -yisK (2X)